Redox Biology 52 (2022) 102296

Contents lists available at ScienceDirect

Redox Biology

journal homepage: www.elsevier.com/locate/redox

Dietary salt initiates redox signaling between endothelium and vascular smooth muscle through NADPH oxidase 4

Kai er Ying [a], Wenguang Feng [a], Wei-Zhong Ying [a], Xingsheng Li [d], Dongqi Xing [a], Yong Sun [c], Yabing Chen [c,e], Paul W. Sanders [a,b,e,*]

[a] Department of Medicine, University of Alabama at Birmingham, Birmingham, AL, 35294-0007, USA
[b] Department of Cell, Developmental and Integrative Biology, University of Alabama at Birmingham, Birmingham, AL, 35294-0007, USA
[c] Department of Pathology, University of Alabama at Birmingham, Birmingham, AL, 35294-0007, USA
[d] Department of Urology, University of Alabama at Birmingham, Birmingham, AL, 35294-0007, USA
[e] Birmingham Department of Veterans Affairs Health Care System, Birmingham, AL, 35233, USA

ARTICLE INFO

Keywords:
Vascular smooth muscle
Cell signaling
Hydrogen peroxide
Runx2
Dietary salt

ABSTRACT

Prevention of phenotype switching of vascular smooth muscle cells is an important determinant of normal vascular physiology. Hydrogen peroxide (H_2O_2) promotes osteogenic differentiation of vascular smooth muscle cells through expression of Runt related transcription factor 2 (Runx2). In this study, an increase in dietary NaCl increased endothelial H_2O_2 generation through NOX4, a NAD(P)H oxidase. The production of H_2O_2 was sufficient to increase Runx2, osteopontin and osteocalcin in adjacent vascular smooth muscle cells from control littermate mice but was inhibited in mice lacking endothelial *Nox4*. A vascular smooth muscle cell culture model confirmed the direct involvement of the activation of protein kinase B (Akt) with inactivation of FoxO1 and FoxO3a observed in the control mice on the high NaCl diet. The present study also showed a reduction of catalase activity in aortas during high NaCl intake. The findings demonstrated an interesting cell-cell communication in the vascular wall that was initiated with H_2O_2 production by endothelium and was regulated by dietary NaCl intake. A better understanding of how dietary salt intake alters vascular biology may improve treatment of vascular disease that involves activation of Runx2.

1. Introduction

Vascular smooth muscle cells (VSMC) may undergo significant phenotypic change in association with arterial diseases [1]. Osteoblastic differentiation of VSMC develops with upregulation of Runt related transcription factor 2 (Runx2), the key transcription factor of the Runx family [2]. Expression of Runx2, also known as Core-Binding Factor Subunit Alpha-1 (CBF-alpha-1), has been identified in calcified human vascular tissue specimens, but not in normal vessels [3–5]. By regulating the expression of alkaline phosphatase and bone matrix protein genes, including osteocalcin, osteopontin, collagen type I, and bone sialoprotein [6,7], Runx2 is an essential and sufficient regulator of vascular calcification [8,9] and aortic fibrosis and stiffness [10]. Onset of these vascular changes predicts development of heart failure, myocardial infarction, stroke, and chronic kidney disease [11–17]. Understanding those mechanisms that increase Runx2 and produce osteogenic differentiation of VSMC is therefore an important goal of study.

Ingestion of certain dietary electrolytes, especially sodium and potassium, regulate arterial structure and function. The endothelium may be considered a 'first responder' to the vascular changes resulting from dietary NaCl and potassium intake. Ambient concentrations of potassium regulated endothelial cell function by modifying cell signaling mediated by protein kinase B (Akt) and Phosphatase and tensin homolog (PTEN) [2]. A prior study also demonstrated that dietary potassium

Abbreviations: Runx2, Runt related transcription factor 2, also known as Core-Binding Factor Subunit Alpha-1 (CBF-alpha-1); H_2O_2, hydrogen peroxide; NOX4, NAD(P)H oxidase 4; Akt, protein kinase B; VSMC, vascular smooth muscle cells; PTEN, Phosphatase and tensin homolog; TGF-β1, TGF-beta 1 protein; FoxO1, Forkhead box O class 1; FoxO3a, Forkhead box O class 3a; Pex14, Peroxisomal Biogenesis Factor 14; ANOVA, analysis of variance; HUVEC, human umbilical vein endothelial cells; PI3K, phosphatidylinositol 3-kinase; PP2a, protein phosphatase type 2A; BP, blood pressure.

* Corresponding author. Division of Nephrology, MCLM 452, 1720 Second Avenue South, University of Alabama at Birmingham, Birmingham, AL, 35294-0007, USA.

E-mail address: psanders@uab.edu (P.W. Sanders).

https://doi.org/10.1016/j.redox.2022.102296
Received 4 March 2022; Accepted 16 March 2022
Available online 24 March 2022

regulated the VSMC expression of Runx2 and development of calcification and arterial stiffness in ApoE-deficient mice [18]. Along with potassium, studies have shown that dietary NaCl intake had profound effects on endothelial function in rodents [2,19–23]. The dietary content of NaCl determined aortic stiffness in humans [24,25], but there are gaps in understanding how these vascular changes are regulated. Dietary NaCl activated endothelial cell signaling pathways reminiscent of mechanotransduction mechanisms [26,27], likely from expansion of extracellular fluid volume during high salt intake. Initiation of signaling in the endothelium resulted in production of TGF-beta 1 protein (TGF-β1), which served an autacoid function that produced NAD(P)H oxidase-4 (NOX4) through Smad signaling in endothelium [28].

Hydrogen peroxide (H_2O_2) has gained attention as an important molecule involved in a several signaling pathways that impact cardiovascular physiology, providing adaptation to changes in the environment in normal and pathologic states [29,30]. While H_2O_2 may be derived from several cellular sources [30], the NAD(P)H oxidase family is an important source of superoxide and H_2O_2. NOX4 is a unique NAD(P)H oxidase that is more evolutionarily distant from the other NOX enzymes, preferentially produces H_2O_2, is thought to be constitutively active [31–33], and is the major catalytic component of endothelial NAD(P)H oxidase [34]. In renal proximal tubule epithelium, H_2O_2 promoted cell signaling events that involved phosphatidylinositol 3-kinase (PI3K), protein kinase B (Akt), Forkhead box O class 3a (FoxO3a), and Sirtuin 1; the resultant changes in the activities of these molecules downregulated catalase, a critically important antioxidant enzyme [35]. Another recent study showed that H_2O_2 promoted the phosphorylation of Peroxisomal Biogenesis Factor 14 (Pex14), preventing transport of catalase into peroxisomes [36]. By decreasing catalase and preventing the proper cellular localization of this enzyme, these H_2O_2-dependent events enhanced the other cellular effects of H_2O_2.

Current evidence supported a direct role for H_2O_2 in the expression of Runx2 and subsequent osteogenic differentiation of VSMC [8]. We generated a mouse model that lacked *Nox4* in endothelium (*VE-Cad-Cre*$^{+}$*/Nox4*$^{fl/fl}$ genotype), and compared with their littermate (*VE-Cad-Cre*$^{-}$*/Nox4*$^{fl/fl}$) controls. Our studies revealed that a high-salt diet increased endothelial NOX4, which produced amounts of H_2O_2 sufficient to promote in adjacent VSMC redox signaling events that increased Runx2 and reduced catalase. The findings supported a dietary salt intake-mediated endothelial-VSMC crosstalk that featured redox signaling and produced Runx2 in adjacent VSMC.

2. Material and methods

2.1. Commercial reagents

Recombinant human transforming growth factor-beta 1 protein (TGF-β1) was obtained commercially (Cat# 240B, R&D Systems, Inc., Minneapolis, MN). LY294002 (Cat# 15447-36-6, Selleckchem, Houston, TX), a pharmacological inhibitor of phosphatidylinositol 3-kinase (PI3K) [37], was dissolved in 0.001% DMSO final and used at a concentration of 50 μM. The solvent alone served as the corresponding vehicle controls. Antibodies directed against Akt (pan) (C67E7, Cat# 4691); p-Akt (Ser473) (D9E, Cat# 9271); FoxO1 (C29H4, Cat# 2880); p-FoxO1 (ser256) (Cat# 9461); FoxO3a (75D8, Cat# 2497); p-FoxO3a(Ser253) (D18H8, Cat# 13129); catalase (D4P7B, Cat# 12980) were all obtained from a commercial vendor (Cell Signaling Technology Inc., Danvers, MA). Experiments also used commercial antibodies directed against FoxO1 (Cat# NB100-2312, Novus Biologicals, Centennial CO); p-FoxO1 (ser256) (Cat# NB100-81927, Novus Biologicals), Runx2 (Cat# ab23981, Abcam Inc., Cambridge, MA), Runx2 (C-12) (Cat# sc-390715, Santa Cruz Biotechnology, Inc., Dallas, TX), PP2A (clone 1D6, Cat# 05–421, Millipore, Temecula, CA), osteopontin (Cat# ab283656, Abcam Inc., Cambridge, MA), osteocalcin (Cat# ab133612, Abcam Inc., Cambridge, MA), and GAPDH (Cat# Ab8245; Abcam Inc., Cambridge, MA), which served as a loading normalization control. Secondary antibodies used for western analyses included Alexa Fluor AffiniPure 680-conjugated goat anti-rabbit antibody (Cat# 712-625-150); goat anti-mouse IgG (Cat# 115-625-146); Alexa Fluor 790-conjugated goat anti-rabbit antibody (Cat# 111-655-144); and goat anti-mouse IgG (Cat#115-655-146); all were obtained from Jackson ImmunoResearch Laboratores, Inc., West Grove, PA.

2.2. Animal and tissue preparation

This study was carried out in accordance with the recommendations in the National Institutes of Health (NIH) Guide for the Care and Use of Laboratory Animals. The Institutional Animal Care and Use Committee at the University of Alabama at Birmingham approved the project. Details on the generation of mice used in this study were included in the Supplement. Studies were conducted using 52 ten-week-old male endothelial *Nox4*$^{-/-}$ mice (*VE-Cad-Cre*$^{+}$*/Nox4*$^{fl/fl}$) and littermate controls (*VE-Cad-Cre*$^{-}$*/Nox4*$^{fl/fl}$).

The protocol that was followed has been standardized in our laboratory [28]. The mice were housed under standard conditions and given formulated diets (AIN-76A, Dyets, Inc., Bethlehem, PA) that contained 0.3% or 4.0% NaCl. Four groups of mice were studied: *VE-Cad-Cre*$^{+}$*/Nox4*$^{fl/fl}$ (endothelial *Nox4*$^{-/-}$) mice received either 0.3% or 4% NaCl diet; littermate *VE-Cad-Cre*$^{-}$*/Nox4*$^{fl/fl}$ mice received either 0.3% or 4% NaCl diet. Blood pressure was recorded and analyzed using DSI radiotelemetric system (DSI, Saint Paul, MN) as previously described [28]. Briefly, mice were anesthetized using isoflurane. Left carotid artery was exposed. The catheter of a PA-C10 transmitter was inserted into the carotid artery reached to aorta, and the transmitter body was placed at the left flank subcutaneously. The mice were allowed to recover for one week before experiments. Blood pressure of both strains of mice was monitored during 0.3% NaCl diet intake as baseline, then switched to 4% NaCl diet intake for 28 days.

On the 28th day of the study, mice were sacrificed and aortic tissues were harvested. Parts of the tissues were homogenized and sonicated in Pierce RIPA buffer (Cat# 89901, Thermo Fisher Scientific Pierce Protein Research Products, Rockford, IL) with Halt Protease & Phosphatase Inhibitor Cocktail (Cat# 1861284, Thermo Fisher Scientific Pierce Protein Research Products, Rockford, IL). Total soluble protein concentration in lysates was determined using a bicinchoninic acid assay (BCA) kit (Cat# 23227, BCA Protein Assay Reagent Kit, Thermo Fisher Scientific Pierce Protein Research Products, Rockford, IL).

2.3. Histology and immunofluorescence microscopy of aorta

A portion of the aortic tissue (n = 8 animals in each group) was fixed in 4% paraformaldehyde overnight and cryopreserved in 20% sucrose. Embedded tissue was sectioned at 5-μm thickness and underwent standard antigen retrieval methods that included pretreatment with 70% ethanol at −20 °C for 10 min. Autofluorescence was reduced by incubation in 50 mM ammonium chloride in PBS for 15 min. Nonspecific staining in the sections was blocked by incubation in 2% normal horse serum in PBS for 1 h, followed by incubation with specific primary antibodies (mouse anti-Runx2 antibody, D130-3, MBL International, Woburn, MA; and rabbit anti-smooth muscle actin, anti-SMA, ab5694, Abcam Inc., Cambridge, MA) overnight at 4 °C. The sections were washed and incubated with the respective secondary antibodies conjugated with Alexa Fluor 488 (green, Invitrogen) and Alexa Fluor 594 (red, Invitrogen). Counterstaining of the nucleus was achieved by mounting sections with hardset mounting media containing DAPI (blue, Vector Laboratories). Negative controls by omission of primary antibody were included in each experiment. Images were acquired using a Leica DM6000 epifluorescence microscope (Leica Microsystems, Bannockburn, IL).

2.4. Dose-dependent effect of TGF-β1 on H_2O_2 production by endothelial cells

Rat aortic endothelial cells and the EC growth medium MCDB-131C were purchased from VEC Technologies (Cat# RAEC/T-75, Cat# MCDB-131C). Human umbilical vein endothelial cells (HUVEC) (Cat# CRL-1730, ATCC, Manassas, VA) were grown in complete F–12K medium (Cat# 30–2004, ATCC) with 10% serum, 0.1 mg/ml of heparin (Sigma, Cat# H3393) and Endothelial Cell Growth Supplement (Cat#. CB-40006, Fisher Scientific, Middletown, VA). Cells were seeded in a 24 well plate. Before treatment with TGF-β1, (Cat# 240B, R&D Systems, Inc., Minneapolis, MN), confluent cells were fasted were fasted for 6 h in EC growth medium, or in F–12K medium without serum. Cells were treated with supplemental TGF-β1 at 0, 0.3, 1, 3, 10, 20 ng/ml for 16 h. After treatment, cells were washed with PBS, and incubated with Amplex® Red reaction mixture (300 μl/well, 0.1 U horseradish peroxidase in 1x reaction buffer) for 1 h. The reaction mixtures were collected and fluorescence determined using an excitation wavelength of 535 nm and emission detected at 590 nm (Spectramax M2e Microplate Reader; Molecular Devices, Sunnyvale, CA). Live cells were counted from the same well with a Scepter Handheld Automated cell Counter (Cat#, PHCC00000, Millipore Corp. Billerica, MA).

2.5. Human smooth muscle cell culture

Human aortic smooth muscle cells were obtained commercially (Cat# 354-05A, Sigma-Aldrich Corp. St Louis, MO). Monolayers of VSMC were grown on 6-well plates or 100 mm dishes (Corning-Costar, Corning Life Sciences) and incubated at 37 °C with 10% CO_2 and 95% air atmosphere in Dulbecco's Modified Eagle Medium (DMEM) (Cat# 10567-014, Gibco, Thermo Fisher Scientific) supplemented with 10% fetal bovine serum. Medium was exchanged at 48-h intervals, and the cells were used between the 4th and 6th subpassage.

In some studies, at the start of the experiment, confluent VSMC were washed and pretreated with 50 μM LY294002 (Cat# s1105 Selleckchem) in serum-free medium (DMEM) for 30 min, and then exposed for 24 h medium containing 0, or 0.4 mM H_20_2. Dilution of H_2O_2 was accomplished using a 30% stock solution (Cat# H1009, Sigma-Aldrich, St. Louis, MO). Control group (without H_2O_2) was incubated under the same conditions. The dose of H_2O_2 chosen for these experiments was within the concentration range (0.2–1 mM) of reactive species reported by other investigators [38–41] and shown to be sufficient to produce VSMC calcification in vitro [8]. Following incubation, the medium was harvested promptly for assays and cells were collected and lysed in radioimmunoprecipitation (RIPA) buffer or buffer from commercial assay kits. The lysis buffer contained a protease inhibitor cocktail (Cat# 1861284, Pierce Halt Protease and Phosphatase inhibitor, Thermo Scientific, Rockford, IL). Cell supernatants and cell lysates were clarified by centrifugation and stored at −70 °C until assayed.

2.6. Silencing catalase, FoxO1, and FoxO3a in vitro incubation studies

RNA interference was accomplished using Catalase Human siRNA Oligo Duplex (Locus ID 847, OriGene Technologies Inc., Rockvile, MD), SignalSilence® FoxO1 siRNA I (Cat# 6242, Cell Signaling Technology, Danvers, MA), and SignalSilence® FoxO3a siRNA I (Cat# 6302, Cell Signaling Technology, Danvers, MA); Trilencer-27 universal scrambled negative siRNA (Cat# SR30004, OriGene Technologies Inc.) served as a control in these experiments. VSMC at 80% confluence were transfected using siTran 2.0 Transfection reagent (Cat# TT320002, OriGene Technologies Inc.) containing the siRNA. Catalase siRNA Oligo Duplex (10 nM), SignalSilence® FoxO1 siRNA I (100 nM), and SignalSilence® FoxO3a siRNA I (100 nM) were complexed with 2.4 μl of siTran 2.0 Transfection reagent in 100-μl of transfection buffer and then added to complete medium in a final volume of 1 ml for each well in a 6-well plate. After incubation in the transfection solution for 48 h, cells were then incubated in medium that contained 0 mM, or 0.4 mM H_2O_2 for an additional 24 h. Cells were then harvested by gentle scraping and centrifugation at 300×*g* for 10 min at 4 °C and resuspended in PBS. Cell lysates were obtained for analysis of catalase activity, PP2a activity, Runx2 ELISA, total protein concentration, or western blotting for Akt, p-Akt, p-FoxO3a, FoxO3a, p-FoxO1, p-FoxO1, catalase, Runx2, and GAPDH.

2.7. Quantification of H_2O_2

H_2O_2 was quantified using a kit (Amplex® Red Hydrogen Peroxide/Peroxidase Assay Kit, Molecular Probes), following the protocol provided by the manufacturer. Medium or serum samples, which were diluted 1:10 in reaction buffer, and standards were mixed with the working solution and incubated at room temperature for 30 min, protected from light. Fluorescence was excited at 535 nm and emission detected at 590 nm (Spectramax M2e Microplate Reader; Molecular Devices, Sunnyvale, CA). All samples were tested in duplicate and averaged.

To quantify the effect of catalase knockdown on cell content of H_2O_2, 48 h after transfection using either siRNA that targeted catalase or nontargeting siRNA, VSMC were then incubated in serum-free medium that contained 0 mM or 0.4 mM H_2O_2 for 5, 10, 15, 20, and 30 min. At each time point, medium was removed and cells were washed with PBS, then incubated with Amplex® Red reaction mixture (150 μl/well, 0.1 U horseradish peroxidase in 1x reaction buffer) for 1 h. Fifty μl of the reaction mixture was collected for each assay and fluorescence determined using an excitation wavelength of 535 nm and emission detected at 590 nm (Spectramax M2e Microplate Reader; Molecular Devices, Sunnyvale, CA). Live cells were counted from the same well with a Scepter Handheld Automated cell Counter (Cat#, PHCC00000, Millipore Corp. Billerica, MA).

2.8. Western blot analyses

Tissue and cell lysates (20–60 μg total protein) were boiled for 5 min in Laemmli buffer and separated using 7–12% SDS-PAGE (Cat# 5671044 Bio-Rad Laboratories, Hercules, CA), before electrophoretic transfer onto PVDF membranes. The membranes were blocked in 5% nonfat milk and then probed with an antibody (diluted 1:1000) that recognized specifically catalase, FoxO1, pFoxO1(ser256); FoxO3a, pFoxO3a(S253), Akt(pan), pAkt(S473), Runx2, PP2A, osteopontin, osteocalcin, and GAPDH (diluted 1:5000). After washes, the blots were incubated for 1 h at room temperature with Alexa Fluor 680 or 790 conjugated AffiniPure anti-rabbit or anti-mouse secondary antibody (1:10,000 dilution). The bands were detected using the Odyssey CLx Infrared Imaging System (LI-COR Biosciences, Lincoln, NE), and densitometric analysis was performed using Image Studio Software (LI-COR Biosciences, Lincoln, NE).

2.9. Quantification of human Runt related transcription Factor2 (Runx2)

Cell Lysates levels of Runx2 were also determined using ELISA (Cat# MB3452519, MyBioSource, Inc. San Diego, CA), following the protocol provided by the manufacturer. Collected cells were washed and resuspend in PBS and then ultrasonicated. Cell lysates were centrifuged at 1500×*g* for 10 min to remove cellular debris. 100 μl of cell lysates and a dilution of each standard were added to an antibody-coated 96-well plate and incubated at 37 °C for 2 h 100 μl of Detection Reagent A were added into each well. The plate was incubated at 37 °C for 1 h. After washing, 100 μl of Detection Reagent B was added into each well. The plate was incubated at 37 °C for 1 h, followed by substrate and stop solution. Runx2 levels were quantified using a colorimetric plate reader (Spectramax M2e Microplate Reader; Molecular Devices, Sunnyvale, CA).

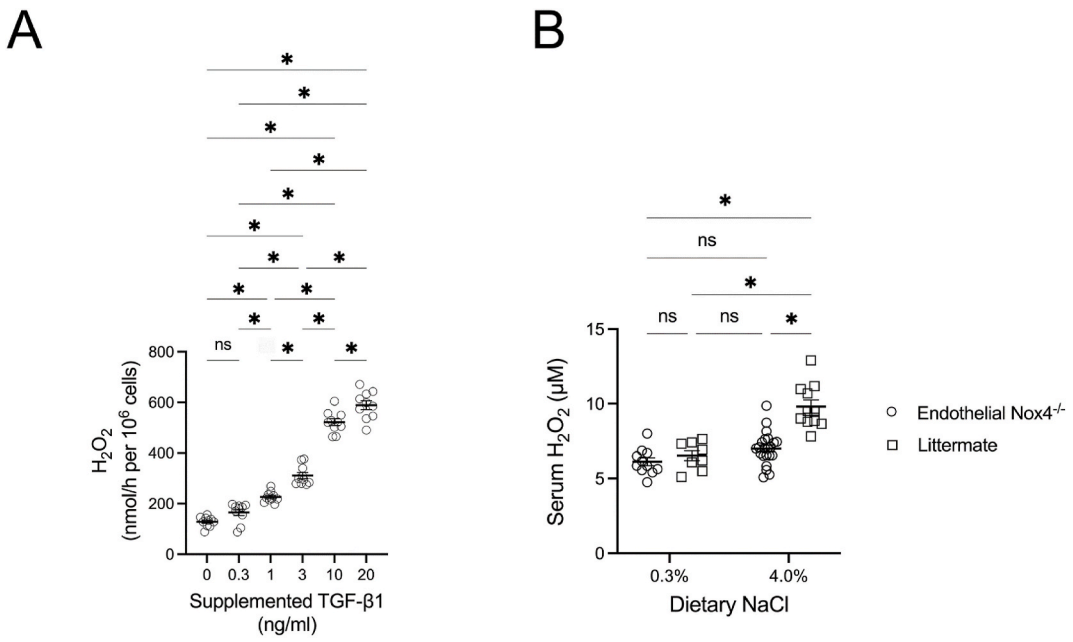

Fig. 1. Endothelial cells produce H_2O_2. **A**, HUVEC incubated overnight in medium that contained active TGF-β in concentrations between 0 (vehicle alone, 4 μM HCl) and 20 ng/ml demonstrated a dose-dependent increase in medium H_2O_2 concentration detected using Amplex® Red. (n = 10 experiments in each group; ns, not significant; *$P < 0.05$; one-way ANOVA) **B**, While on a diet that contained 0.3% NaCl, mice that lacked *Nox4* in endothelium (*VE-Cad-Cre*$^{+}$/*Nox4*$^{fl/fl}$) (n = 11 mice) and littermate (*VE-Cad-Cre*$^{-}$/*Nox4*$^{fl/fl}$) controls (n = 8 mice) demonstrated similar concentrations of H_2O_2 in the serum. When placed on the diet containing 4.0% NaCl, serum levels of H_2O_2 increased ($P < 0.05$) in the littermate controls (n = 11 mice), when compared to the other three groups, but did not increase ($P > 0.05$) in the endothelial *Nox4*$^{-/-}$ mice (n = 22 mice). The analysis also showed significant effects of *Nox4* ($P < 0.05$) and dietary salt ($P < 0.05$) on serum H_2O_2 as well as an interaction effect ($P < 0.05$) between *Nox4* and dietary salt. (ns, not significant; *$P < 0.05$; Two-way ANOVA).

2.10. Determination of catalase activity

Catalase activity was quantified using a commercially available kit (Catalase Colorimetric Activity Assay Kit, Cat# EIACATC, Invitrogen by Thermo Fisher Scientific, Frederick, MD). VSMC at 1×10^6 were resuspended in cold 1X assay buffer and homogenized on ice by sonication, following the protocol provided by the manufacturer. The reaction included hydrogen peroxide, substrate, and HRP solution. Colorimetric absorbance was read at 560 nm. (Spectramax M2e Microplate Reader; Molecular Devices, Sunnyvale, CA). All samples were tested in duplicate and averaged.

2.11. Protein phosphatase 2 (PP2a) activity assay

PP2a activity was assayed using a PP2A Immunoprecipitation Phosphatase Assay Kit, (Cat# 17–313, Millipore, Temecula, CA), following the manufacturer's protocol. Treated VSMC at 2×10^6 were resuspend in 0.3 ml of phosphatase extraction buffer, containing 20 mM imidazole HCl, 2 mM EGTA, pH 7.0, with 10 μg/ml each of aprotinin, leupeptin, and pepstatin, and 1 mM benzamidine and 1 mM phenylmethylsulfonyl fluoride. The cells were homogenized and centrifuged at 2000×*g* for 5 min. Total protein concentration of the supernatants was determined using a BCA Protein Assay Reagent Kit (Cat# 23227, Pierce Protein Research Products, Thermo Fisher Scientific), and 250 μg of lysate were used for each phosphatase activity assay. Cellular lysates were immunoprecipitated with 4 μg of anti-PP2a, C subunit antibody (clone 1D6, Cat# 05–421, Millipore) and 40 μl of Protein A agarose slurry for 2 h at 4 °C. Following washes, phosphatase substrate was added. After a 10-min development time, absorbance was read at 650 nm using a microplate reader (Spectramax M2e Microplate Reader; Molecular Devices, Sunnyvale, CA). Absorbance was compared to the standard curve to determine PP2a activity. Along with determination of PP2a activity, western analysis of the immunoprecipitates was performed using the same antibody that was directed against the catalytic subunit of anti-PP2a.

2.12. Statistics

All data including those represented graphically were expressed as mean ± SEM. For multiple group comparisons, either one-way analysis of variance (ANOVA) or two-way ANOVA, followed by Tukey's multiple comparisons test, was performed using Prism, version 9.2.0. Two-way ANOVA partitioned the overall variance of the outcome variable into three components, plus a residual (or error) term. It computed *P* values that tested three null hypotheses: an interaction *P* value for the null hypothesis that there was no interaction between the two factors on the response, as well as *P* values for the null hypotheses that each factor had no effect on the response. Where appropriate, *P* values that tested the null hypotheses were provided in the figure legends, while significance demonstrated through subsequent post-hoc testing was illustrated with asterisks within the figure. $P < 0.05$ was considered statistically significant.

3. Results

3.1. Endothelium produced H_2O_2 in response to TGF-β1 in vitro and increased dietary salt intake in vivo

Consistent with our prior finding that increased dietary NaCl intake activated endothelial TGF-β signaling, which was upstream of NOX4 [28], overnight incubation of human umbilical vein endothelial cells (HUVEC) in medium containing supplemental TGF-β1 produced a dose-dependent increase in H_2O_2 release (Fig. 1A). Primary cultures of aortic endothelial cells also demonstrated this dose-dependent response to the addition of TGF-β1 into the medium (Supplemental Fig. 1). These findings were also compatible with studies from other investigators showing that TGF-β increased production of H_2O_2 through NOX4 in arterial beds [42–46]. While on a diet that contained 0.3% NaCl,

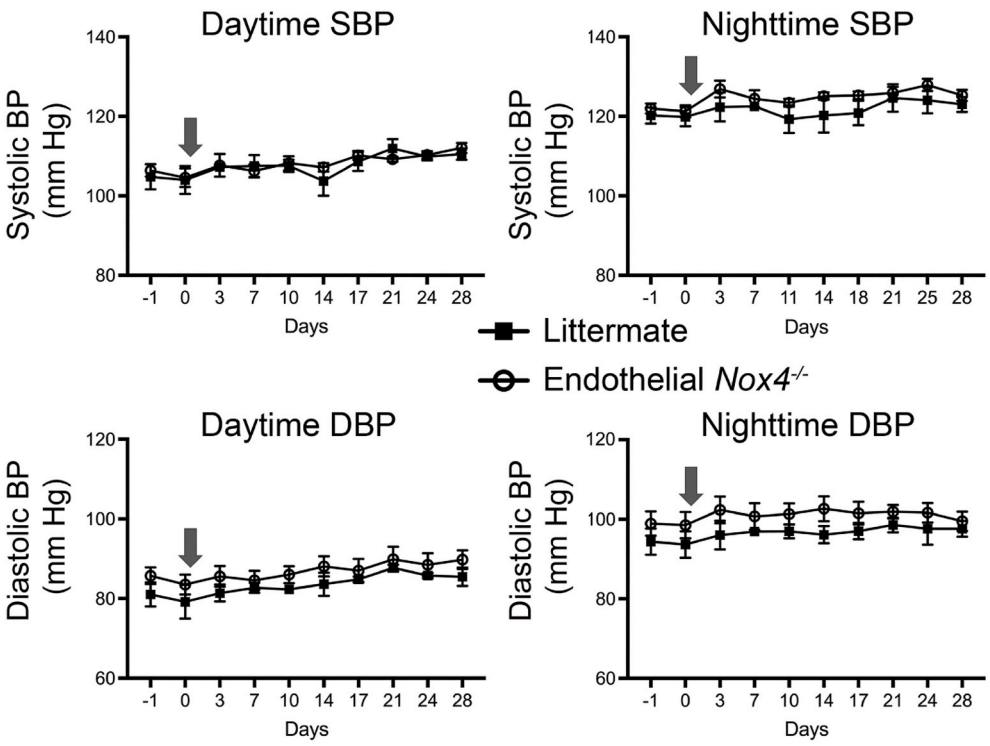

Fig. 2. Comparison of telemetry-monitored unrestrained blood pressures. Daytime and nighttime systolic (SBP) and diastolic (DBP) blood pressures of mice that lacked *Nox4* in endothelium (*VE-Cad-Cre*$^{+}$/*Nox4*$^{fl/fl}$) (n = 5 mice) and littermate (*VE-Cad-Cre*$^{-}$/*Nox4*$^{fl/fl}$) controls (n = 3 mice) did not differ either at baseline on a 0.3% NaCl diet (days −1 and 0) or when fed a 4.0% NaCl diet (days 1 through 28). Arrow on graphs indicate the time of change in the diet from 0.3% NaCl to 4.0% NaCl.

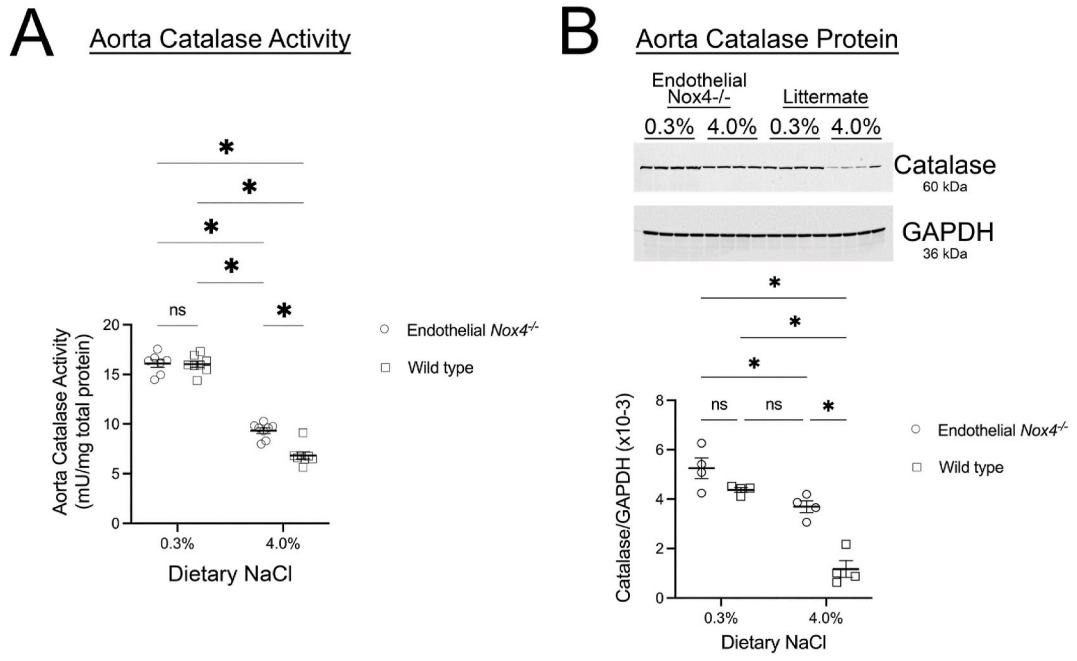

Fig. 3. Catalase activity and protein content in aortas of endothelial *Nox4*$^{-/-}$ and littermate mice with changes in dietary salt content. A, During ingestion of the 0.3% NaCl diet, catalase activity in the aorta did not differ between the strains. When fed a 4.0% NaCl diet, catalase activity fell in both strains but to a greater ($P < 0.05$) extent in the littermate control mice. **B,** During ingestion of the 0.3% NaCl diet, catalase protein content in the aorta did not differ between the strains. When fed a 4.0% NaCl diet, catalase activity fell in both strains but to a greater ($P < 0.05$) extent in the littermate control mice. Two-way ANOVA showed significant effects of *Nox4* ($P < 0.05$) and dietary salt ($P < 0.05$) on catalase activity and protein content and an interaction effect ($P < 0.05$) between *Nox4* and dietary salt. (n = 4 mice in each group; ns, not significant; *$P < 0.05$; Two-way ANOVA).

endothelial *Nox4*$^{-/-}$ and littermate (*VE-Cad-Cre*$^{-}$/*Nox4*$^{fl/fl}$) control mice demonstrated similar concentrations of H_2O_2 in the serum (Fig. 1B). When fed the diet containing 4.0% NaCl, serum levels of H_2O_2 increased ($P < 0.05$) in the littermate controls, when compared to the other three groups, but did not increase ($P > 0.05$) in the endothelial *Nox4*$^{-/-}$ mice. These studies identified endothelial NOX4 as the source of increased H_2O_2 levels during increased NaCl intake. This effect was independent of changes in arterial pressures, since telemetry-monitored blood pressures did not differ between the *VE-Cad-Cre*$^{+}$/*Nox4*$^{fl/fl}$ and *VE-Cad-Cre*$^{-}$/*Nox4*$^{fl/fl}$ mice during ingestion of the 4% NaCl diet (Fig. 2).

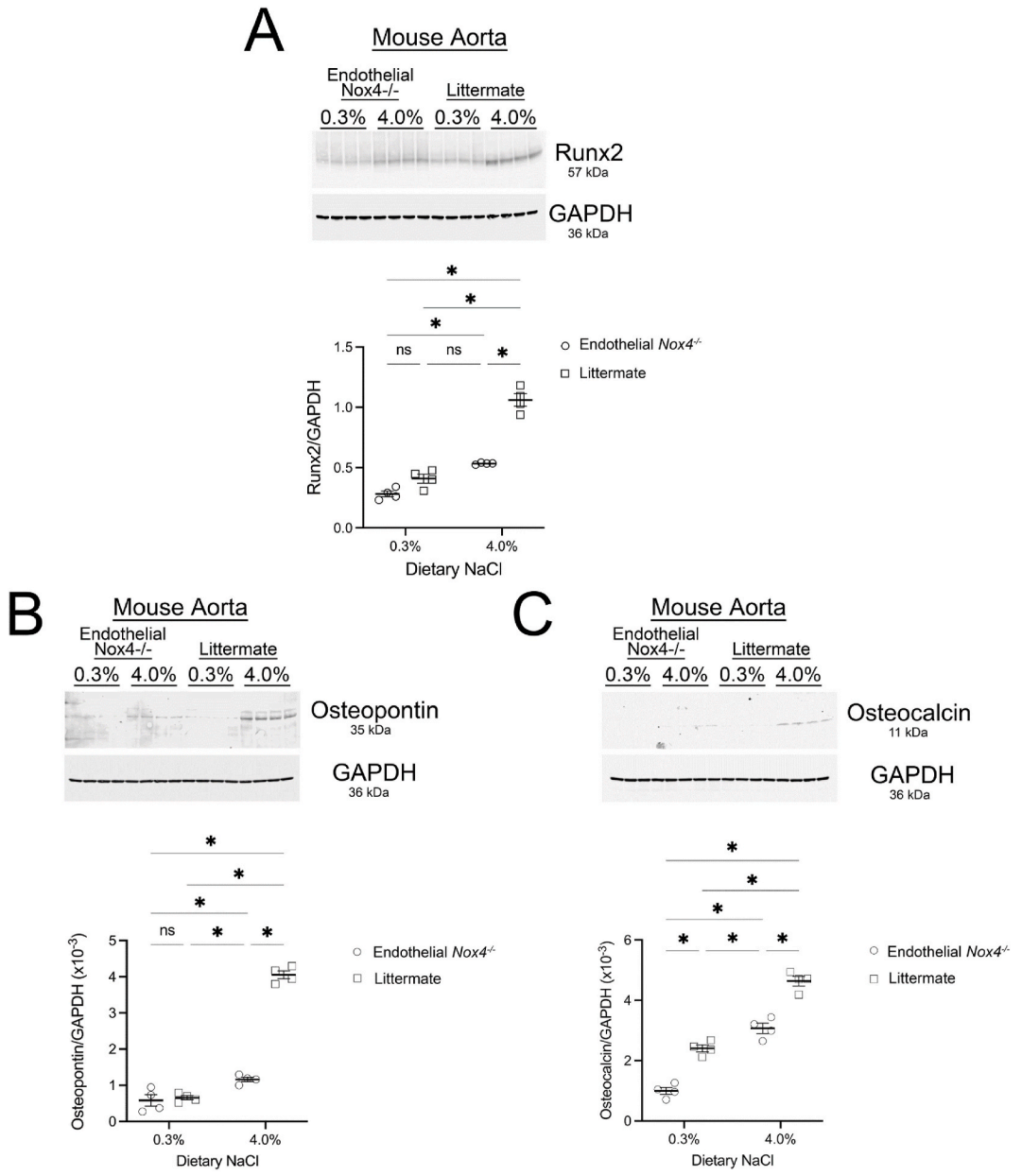

Fig. 4. Western analysis of aortic content of Runx2, osteopontin, and osteocalcin of endothelial *Nox4*$^{-/-}$ and littermate mice with changes in dietary salt content. A, During ingestion of the 0.3% NaCl diet, Runx2 levels in the aorta did not differ between the strains. When fed a 4.0% NaCl diet, Runx2 increased in the aortas of littermate mice, when compared with the endothelial *Nox4*$^{-/-}$ mice. Two-way ANOVA showed significant effects of *Nox4* ($P < 0.05$) and dietary salt ($P < 0.05$) on catalase activity and Runx2 and an interaction effect ($P < 0.05$) between *Nox4* and dietary salt (n = 4 mice in each group; ns, not significant; *$P < 0.05$; Two-way ANOVA). **B**, When fed a 4.0% NaCl diet, osteopontin increased in the aortas of littermate mice, when compared with the endothelial *Nox4*$^{-/-}$ mice. Two-way ANOVA showed significant effects of *Nox4* ($P < 0.05$) and dietary salt ($P < 0.05$) on osteopontin and an interaction effect ($P < 0.05$) between *Nox4* and dietary salt (n = 4 mice in each group; ns, not significant; *$P < 0.05$; Two-way ANOVA). **C**, When fed a 4.0% NaCl diet, osteocalcin increased in the aortas of littermate mice, when compared with the endothelial *Nox4*$^{-/-}$ mice. Two-way ANOVA showed significant effects of *Nox4* ($P < 0.05$) and dietary salt ($P < 0.05$) on osteopontin, but no interaction effect ($P = 0.5943$) between *Nox4* and dietary salt (n = 4 mice in each group; *$P < 0.05$; Two-way ANOVA).

3.2. Endothelium-Nox4$^{-/-}$ *mice were protected from NaCl-induced activation of Runx2 in VSMC*

Because of the known inhibitory effects of H_2O_2 and other reactive species on catalase protein levels [35] and activity [47–49], initial studies determined catalase activity in aortic lysates from mice on the low salt (0.3%) or high salt (4.0%) diet for 30 days. Aorta catalase activity levels did not differ ($P > 0.05$) between endothelial *Nox4*$^{-/-}$ mice and littermate controls on the 0.3% NaCl diet. In the 4.0% NaCl groups, catalase activity fell in both strains but to a greater ($P < 0.05$) extent in the littermate control mice (Fig. 3A). In a similar fashion, Western analysis of the relative content of catalase in the aorta showed a pattern like the catalase activity findings (Fig. 3B). Western analysis of aortic lysates from endothelial *Nox4*$^{-/-}$ and littermate control mice given either a low salt (0.3%) or high salt (4.0%) diet for 30 days showed similar amounts of Runx2 in the low salt groups; however, aortic lysates of endothelial *Nox4*$^{-/-}$ mice contained less ($P < 0.05$) Runx2 in the high salt groups (Fig. 4A). With the increase in dietary salt intake, two bone matrix proteins – osteocalcin and osteopontin - that were regulated by Runx2 [6,7] also increased in the littermate controls, but were lower in the endothelial *Nox4*$^{-/-}$ mice (Fig. 4B and C). Consistent with the western analyses, immunohistochemistry of aortas from endothelial

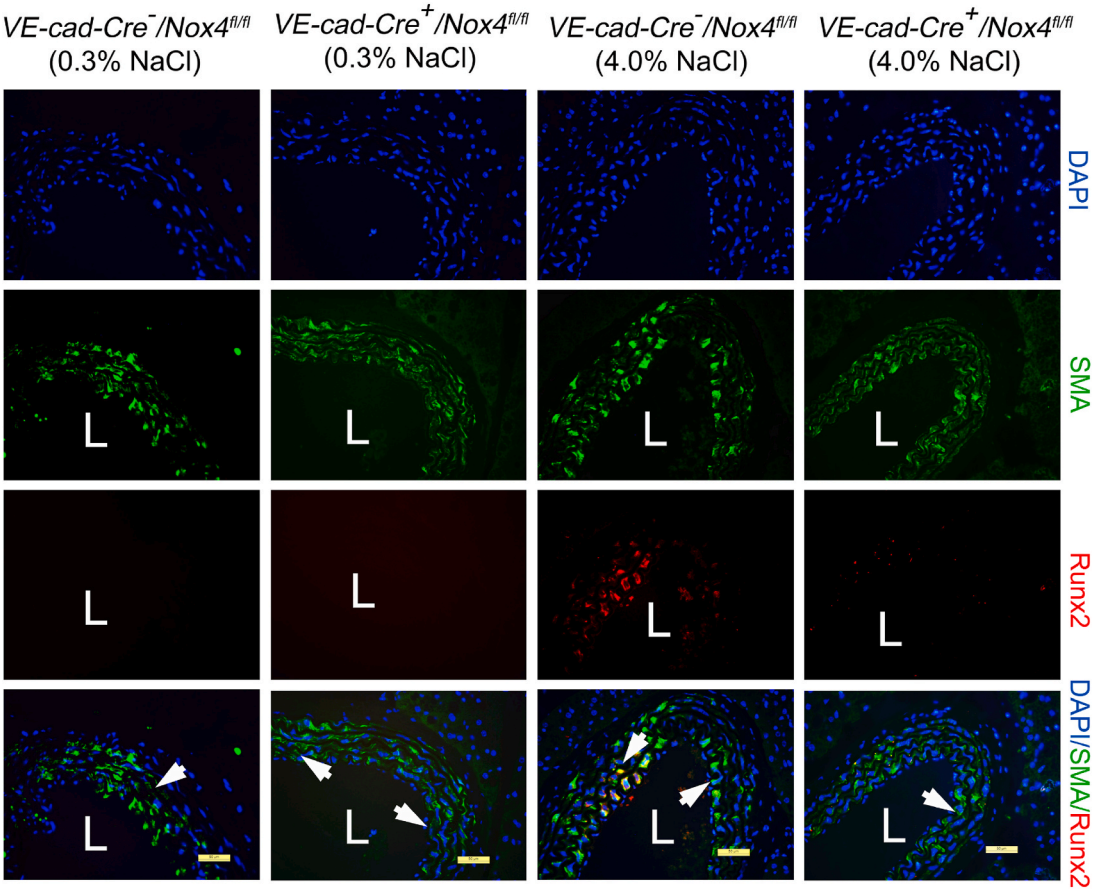

Fig. 5. Immunohistochemistry analysis of expression of Runx2 in the aorta. The smooth muscle cell layers were identified using antibody to SMA (green color). Runx2 was identified using anti-Runx2 antibody (red color). Nuclei were counterstained with DAPI (blue color). While on the 0.3% NaCl diet, aortas of endothelial *Nox4*$^{-/-}$ (*VE-Cad-Cre*$^{+}$/*Nox4*$^{fl/fl}$) and littermate (*VE-Cad-Cre*$^{-}$/*Nox4*$^{fl/fl}$) mice demonstrated no discernible amounts of Runx2 with immunohistochemistry. When fed a 4.0% NaCl diet, Runx2 increased in vascular smooth muscle (arrows) of the aortas of littermate mice. Bar represented 50 μm. L, lumen. (For interpretation of the references to color in this figure legend, the reader is referred to the Web version of this article.)

Nox4$^{-/-}$ and littermate control mice demonstrated minimal expression of Runx2 when maintained on 0.3% NaCl. Runx2 was identified in VSMC of littermate control mice on the 4.0% NaCl diet for 30 days. In contrast, Runx2 was not identified in VSMC of endothelial *Nox4*$^{-/-}$ mice on the 4.0% NaCl diet (Fig. 5).

3.3. Dietary NaCl-induced activation of Akt, FoxO1, and FoxO3a was prevented in aortas of endothelial *Nox4*$^{-/-}$ mice

Western analyses of aortic lysates of endothelial *Nox4*$^{-/-}$ and littermate control mice on 0.3% NaCl and 4.0% NaCl were studied for activity levels of Akt, FoxO1 and FoxO3a; both FoxO1 and FoxO3a have been shown to be phosphorylation targets of Akt [50–52]. When fed the 4.0% NaCl diet, aortic lysates of littermate control mice contained increased levels of phosphorylated Akt and both FoxO1 and FoxO3a, but was limited in lysates from endothelial *Nox4*$^{-/-}$ mice (Fig. 6).

3.4. Inhibition of Akt prevented H_2O_2-mediated changes in pFoxO1, pFoxO3, Runx2, and catalase in VSMC

To provide additional mechanistic findings, human aortic smooth muscle cells (VSMC) were studied in vitro. VSMC cells were incubated initially for 30 min in medium containing either LY294002, a pharmacological inhibitor of phosphatidylinositol 3-kinase (PI3K) [37], or PBS control. H_2O_2, 0.4 mM, or vehicle alone was then added to the medium and the incubation continued overnight. H_2O_2 increased pAkt(S473) in VSMC, while LY294002 inhibited the activation of Akt (Fig. 7A). H_2O_2 increased phosphorylated FoxO1 (pFoxO1(S256)) and FoxO3a (pFoxO3a(S253)) in VSMC, and addition of LY294002 prevented these increases (Fig. 7B and C). Addition of H_2O_2, 0.4 mM, into medium increased VSMC Runx2, which was prevented by LY294002 (Fig. 7D). Addition of H_2O_2, 0.4 mM, into medium of VSMC decreased catalase and catalase activity in lysates of VSMC; the addition of LY294002 mitigated the decrease in catalase and catalase activity (Fig. 7E and F). The results demonstrated that a pivotal role of the PI3K/Akt pathway in mediating H_2O_2-induced phosphorylation of FoxO1 and FoxO3a, increases in Runx2, and decreases in catalase.

3.5. FoxO1 and FoxO3a participated in H_2O_2-induced changes in Runx2 in VSMC

Addition of H_2O_2, 0.4 mM, into the medium increased pFoxO1(S256) and pFoxO1(S253) in VSMC (Fig. 7A and C). Knockdown of FoxO1 and FoxO3a in VSMC using siRNA directed against FoxO1 and FoxO3a, respectively, was confirmed (Fig. 8A and C). Under these conditions, basal Runx2 levels and H_2O_2-induced increases in Runx2 were augmented (Fig. 8B and D). The data confirmed a role for both FoxO1 and FoxO3a in the regulation of Runx2 in VSMC and were consistent with a prior publication showing the direct involvement of FoxO1/3 in upregulation of Runx2 and associated vascular calcification in smooth muscle-specific PTEN-deficient mice [51].

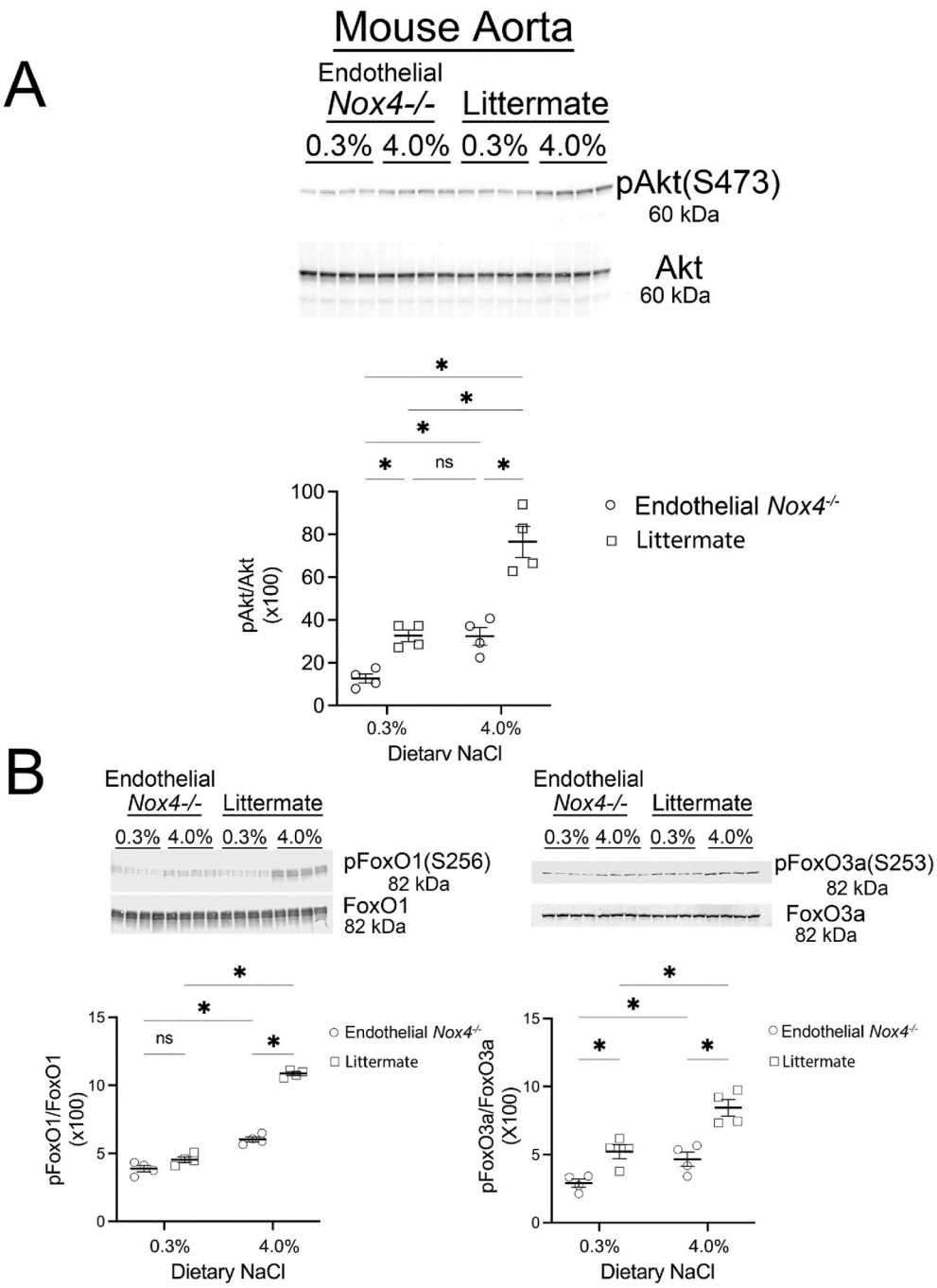

Fig. 6. Western analyses of content of Akt, pAkt, FoxO1, and pFoxO1 in aortic lysates from endothelial *Nox4*$^{-/-}$ and littermate mice fed the 0.3% and 4.0% NaCl diets. A, While on the 0.3% NaCl diet, the endothelial *Nox4*$^{-/-}$ mice demonstrated less Akt activity (pAkt(S473)) ($P < 0.05$) than the littermates. When fed the 4.0% NaCl diet, activation of Akt increased ($P < 0.05$) in the littermate controls. There were significant effects of *Nox4* ($P < 0.05$) and dietary salt ($P < 0.05$) on Akt activation and an interaction effect ($P < 0.05$) between *Nox4* and dietary salt. (n = 4 mice in each group; ns, not significant; *$P < 0.05$; Two-way ANOVA). **B**, Activation of FoxO1 (pFoxO1(S256)) and FoxO3a (pFoxO3a (S253)), two downstream phosphorylation targets of Akt [50,53], increased during the high salt intake. There were significant effects of *Nox4* ($P < 0.05$) and dietary salt ($P < 0.05$) on FoxO1 and FoxO3a activation as well as an interaction effect ($P < 0.05$) between *Nox4* and dietary salt on FoxO1 activation. (n = 4 mice in each group; ns, not significant; *$P < 0.05$; Two-way ANOVA).

3.6. Catalase mitigated H_2O_2-induced changes in PP2a activity and Runx2 in VSMC

Because of the demonstrated decrease in catalase in VSMC incubated in medium containing H_2O_2 (0.4 mM), additional experiments were performed to determine the effect of catalase activity on the upregulation of Runx2. Successful knockdown of catalase in VSMC was performed using siRNA targeting catalase and confirmed using western analysis (Fig. 9A). Cells treated with nontargeting siRNA demonstrated the decrease in catalase when incubated in medium containing 0.4 mM H_2O_2 (Fig. 9A). Catalase activity levels mirrored the western analyses (Fig. 9B). These data were also consistent with the observed effect of H_2O_2 on catalase in the aortas of endothelial *Nox4*$^{-/-}$ mice and littermate controls. To confirm that the catalase knockdown experiments increased available H_2O_2, H_2O_2 accumulation in VSMC pre-treated with siRNA that targeted catalase and nontargeting siRNA was performed over a 30-min period following the addition of H_2O_2 or vehicle alone into the medium (Fig. 9C). VSMC treated with either the catalase or the nontargeting siRNA demonstrated no differences when treated with vehicle alone. VSMC treated with the nontargeting siRNA and incubated with H_2O_2 showed significantly higher levels of H_2O_2 when compared with the vehicle-treated cells, while VSMC treated with the catalase siRNA demonstrated much higher ($P < 0.05$) levels of H_2O_2, compared with the other three groups.

Additional experiments included PP2a, a ubiquitous redox-sensitive phosphatase that is present in smooth muscle [54], is sensitive to H_2O_2 [55,56], and is upstream of the PI3K/Akt pathway [35]. Immunoprecipitation experiments (Fig. 10A) showed similar amounts of the PP2a C subunit in the lysates, but PP2a activity was reduced in the presence of H_2O_2 (Fig. 10B). Loss of catalase further reduced PP2a activity in the

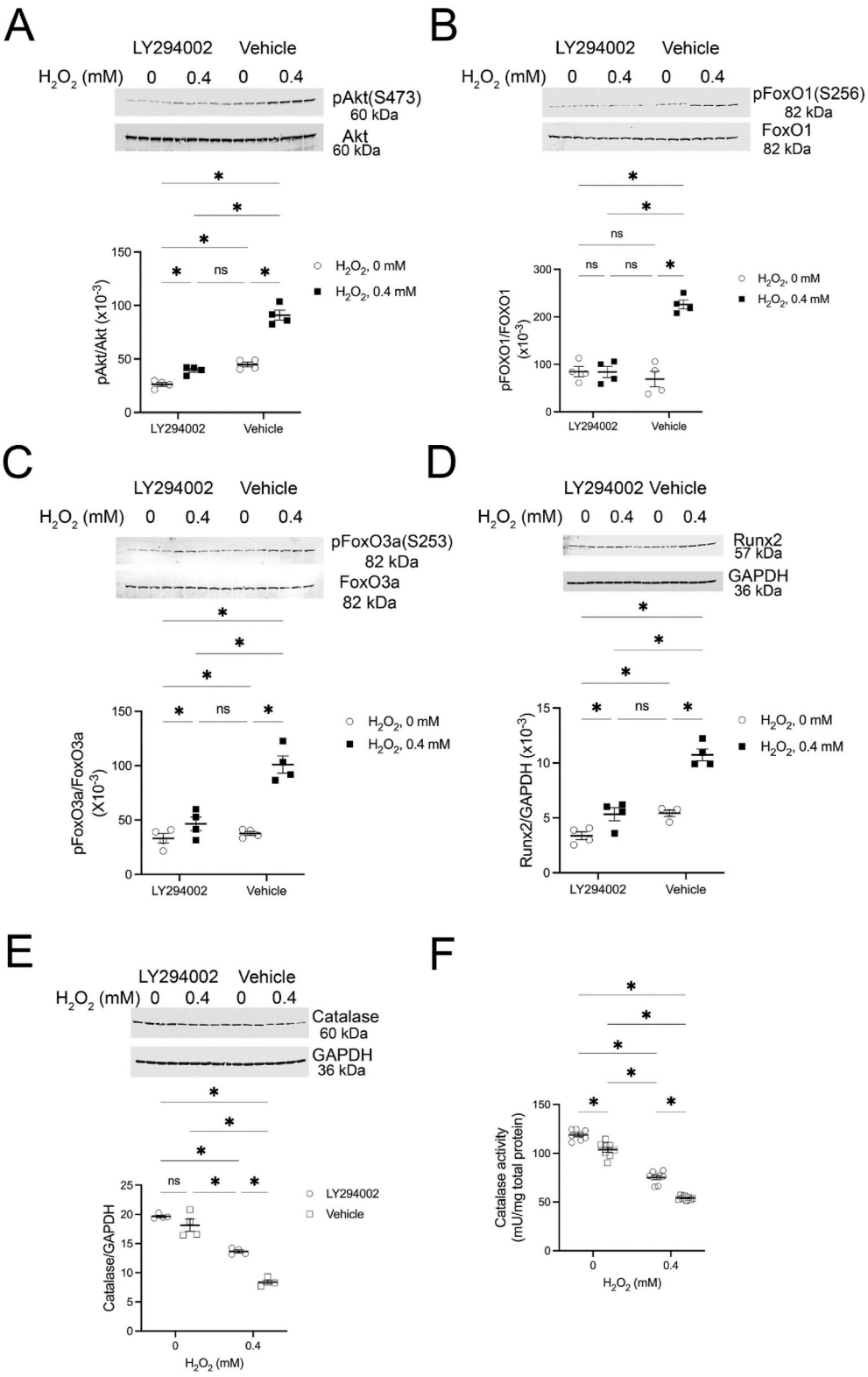

Fig. 7. Inhibition of Akt activation prevented H_2O_2-induced increases in Runx2 and decreases in catalase in vascular smooth muscle cells (VSMC). A, Addition of LY294002, a pharmacological inhibitor of phosphatidylinositol 3-kinase (PI3K) [37], inhibited the activation of Akt during overnight incubation of VSMC in medium containing H_2O_2, 0.4 mM. Both H_2O_2 ($P < 0.05$) and LY294002 ($P < 0.05$) affected Akt activation and an interaction effect ($P < 0.05$) between H_2O_2 and LY294002 on Akt activation was observed. (n = 4 samples in each group; ns, not significant; *$P < 0.05$; Two-way ANOVA) **B** and **C**, Phosphorylated FoxO1 (pFoxO1(S256)) and FoxO3a (pFoxO3a(S253)), two downstream phosphorylation targets of Akt [50,53], increased during incubation of VSMC in medium containing 0.4 mM H_2O_2. The addition of LY294002 inhibited these responses. There were significant effects of H_2O_2 ($P < 0.05$) and LY294002 ($P < 0.05$) on FoxO1 and FoxO3a activation as well as an interaction effect ($P < 0.05$) between H_2O_2 and LY294002 on FoxO1 activation (n = 4 samples in each group; ns, not significant; *$P < 0.05$; Two-way ANOVA). **D**, Addition of H_2O_2, 0.4 mM, into medium increased VSMC Runx2, which was prevented by LY294002. Both H_2O_2 ($P < 0.05$) and LY294002 ($P < 0.05$) affected Runx2 levels and an interaction effect ($P < 0.05$) between H_2O_2 and LY294002 on Runx2 levels was observed (n = 4 samples in each group; ns, not significant; *$P < 0.05$; Two-way ANOVA). **E**, Addition of H_2O_2, 0.4 mM, into medium of VSMC decreased catalase; the addition of LY294002 mitigated this decrease in protein levels. Both H_2O_2 ($P < 0.05$) and LY294002 ($P < 0.05$) affected catalase levels in VSMC and an interaction effect ($P < 0.05$) between H_2O_2 and LY294002 on catalase levels was observed (n = 4 samples in each group; ns, not significant; *$P < 0.05$; Two-way ANOVA). **F**, Consistent with the western analysis data, H_2O_2, 0.4 mM, decreased catalase activity and this effect was mitigated by the addition of LY294002. Both H_2O_2 ($P < 0.05$) and LY294002 ($P < 0.05$) affected catalase activity, but there was no interaction effect ($P = 0.1355$) between H_2O_2 and LY294002 (n = 8 samples in each group; *$P < 0.05$; Two-way ANOVA).

samples (Fig. 10B). The anticipated increase in Runx2 by H_2O_2 was enhanced in samples lacking catalase (Fig. 10C).

4. Discussion

The present studies were the first to demonstrate an interesting redox-mediated communication that developed between the endothelium and VSMC during changes in dietary NaCl intake. Specifically, we demonstrated that an increase in dietary NaCl intake promoted endothelial production of H_2O_2 by NOX4, an unusual NAD(P)H oxidase that produces only H_2O_2 [31,32], and thereby increasing Runx2, along with osteopontin and osteocalcin, and reducing catalase in adjacent VSMC of littermate control mice, but not endothelium-*Nox4*$^{-/-}$ mice. The observations occurred independently of changes in blood

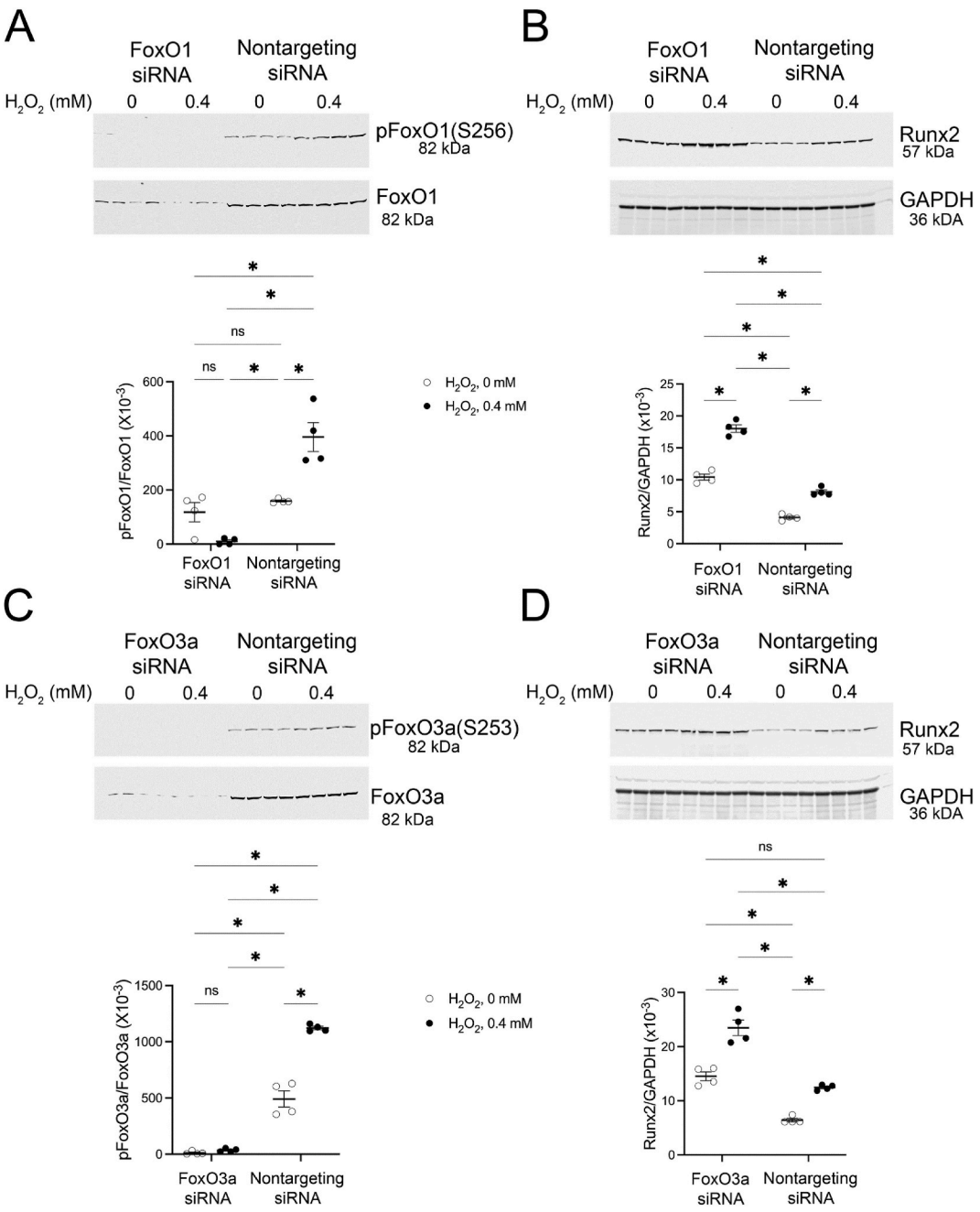

Fig. 8. siRNA-mediated knockdown of FoxO1 or FoxO3a increased basal Runx2 levels and H_2O_2-induced increases in Runx2 in VSMC. A, Western blot showed successful knockdown of FoxO1 by FoxO1-specific siRNA. Addition of H_2O_2 into the medium induced the inhibition of FoxO1 (indicated by the increase in pFoxO1 (S256)). In these studies, FoxO1 siRNA ($P < 0.05$), but not H_2O_2 ($P = 0.07$), affected levels of pFoxO1(S253) in VSMC, but there was an interaction effect ($P < 0.05$) between H_2O_2 and FoxO1 siRNA on pFoxO1(S256). (n = 4 samples in each group; ns, not significant; *$P < 0.05$; Two-way ANOVA) **B,** Knockdown of FoxO1 increased basal expression of Runx2 and increased H_2O_2-mediated increases in Runx2. H_2O_2 ($P < 0.05$) and FoxO1 siRNA ($P < 0.05$) affected levels of Runx2 in VSMC and an interaction effect ($P < 0.05$) between H_2O_2 and FoxO1-specific siRNA on levels of pFoxO1(S256) was observed. (n = 4 samples in each group; *$P < 0.05$; Two-way ANOVA) **C**, Western blot showed successful knockdown of FoxO3a by FoxO3a-specific siRNA. Addition of H_2O_2 into the medium induced the inhibition of FoxO3a (indicated by the increase in pFoxO3a(S253)). In these studies, H_2O_2 ($P < 0.05$) and FoxO3a siRNA ($P < 0.05$) affected levels of pFoxO3a(S253) in VSMC and an interaction effect ($P < 0.05$) between H_2O_2 and FoxO3a siRNA on pFoxO3a(S253) was observed (n = 4 samples in each group; ns, not significant; *$P < 0.05$; Two-way ANOVA). **D**, Knockdown of FoxO3a increased basal expression of Runx2 and increased H_2O_2-mediated increases in Runx2. H_2O_2 ($P < 0.05$) and FoxO3a siRNA ($P < 0.05$) affected levels of Runx2 in VSMC, but an interaction effect ($P > 0.05$) between H_2O_2 and FoxO3a siRNA on levels of pFoxO3a(S253) was not observed (n = 4 samples in each group; ns, not significant; *$P < 0.05$; Two-way ANOVA).

pressure, since telemetry-monitored blood pressures did not differ between the endothelial-*Nox4*$^{-/-}$ mice and littermate controls. The high NaCl diet also promoted activation of Akt, increased phosphorylation of FoxO1 and FoxO3a, and reduced catalase protein and enzymatic activity in the littermate control mice. To provide mechanistic understanding, a series of in vitro studies with VSMC were performed. Incubation of VSMC overnight in medium containing 0.4 mM H_2O_2 showed similar responses with activation of Akt, increased phosphorylation of FoxO1 and FoxO3a, reduced sirtuin 1 activity, and increased Runx2 and decreased catalase activity. The effect on Runx2 was inhibited by the PI3K/Akt inhibitor, LY294002. Knockdown of FoxO1 and FoxO3a increased Runx2 levels. Knockdown of catalase increased Runx2,

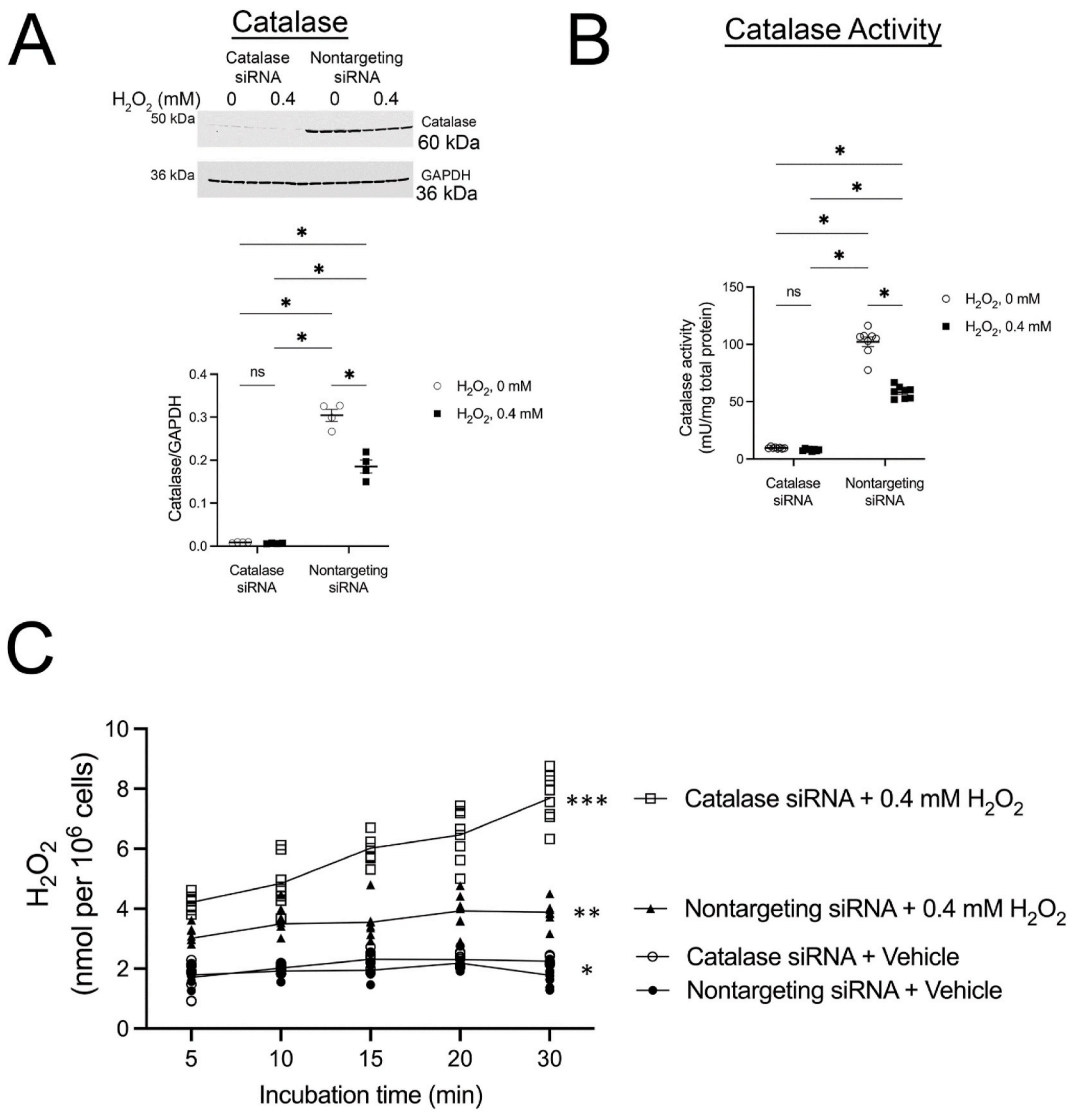

Fig. 9. Effect of siRNA-mediated knockdown of catalase on catalase protein, activity, and bioavailable H_2O_2 in VSMC. A, Western blotting demonstrated successful knockdown of catalase protein by catalase-specific siRNA. Addition of H_2O_2 into the culture medium decreased ($P < 0.05$) levels of catalase in VSMC that received nontargeting siRNA. H_2O_2 ($P < 0.05$) and catalase siRNA ($P < 0.05$) affected catalase protein levels in VSMC and an interaction effect ($P < 0.05$) between H_2O_2 and catalase siRNA on catalase was observed. (n = 4 samples in each group; ns, not significant; *$P < 0.05$; Two-way ANOVA) **B**, Catalase activity followed a similar pattern, with H_2O_2 ($P < 0.05$) and catalase siRNA ($P < 0.05$) affecting catalase activity in VSMC and an interaction effect ($P < 0.05$) between H_2O_2 and catalase siRNA on catalase was observed. (n = 8 samples in each group; ns, not significant; *$P < 0.05$; Two-way ANOVA) **C**, H_2O_2 accumulation during vehicle treatment of VSMC pre-treated with siRNA that targeted catalase and VSMC that received nontargeting siRNA did not differ (*$P > 0.05$). In contrast, incubation of VSMC that received nontargeting siRNA in medium containing H_2O_2, 0.4 mM, showed significant (**$P < 0.05$) increases in H_2O_2 at each time point, compared with the vehicle-treated groups. Incubation in medium containing H_2O_2, 0.4 mM, of VSMC pre-treated with siRNA that targeted catalase produced significantly higher (***$P < 0.05$) amounts of H_2O_2 at each time point, compared with the other three groups in the study. (n = 8 samples in each group; one-way ANOVA).

indicating direct involvement of catalase activity in modifying the effects of these redox signaling events. Supported by the in vitro experiments, the reduction in catalase protein in vivo likely contributed to other events known to reduce catalase activity, including cellular mis-localization of catalase [36] and direct inhibition by other reactive species [47–49]. The combined findings supported a dietary NaCl-mediated endothelial cell-VSMC crosstalk that featured redox signaling originating in endothelium and promoting the expression of Runx2 in VSMC (Fig. 11).

Previous research established a link between high NaCl diet and the development of an endothelial cell signaling pathway that followed activation of transforming growth factor-beta (TGF-β) in rats [19,28]. This autacoid pathway involved an ALK5-dependent increase in endothelial NOX4 [28]. In support of these data and prior observations that endothelial cells have been shown to produce H_2O_2 [42–46], the present studies showed that endothelium produced H_2O_2 in response to TGF-β1 in vitro. Because serum H_2O_2 concentration did not increase in the endothelium-*Nox4*$^{-/-}$ mice during increased NaCl intake, endothelial NOX4 served as the cellular source of this increase in serum H_2O_2 levels. The release of H_2O_2 by endothelium permitted function as a diffusible signaling molecule that impacted vascular adaptation during high dietary NaCl intake.

A direct role for H_2O_2 in the expression of Runx2 and subsequent osteogenic differentiation of VSMC has been identified [8]. However, the mechanism by which H_2O_2 regulated cellular Runx2 and subsequent osteogenic differentiation was complicated. Mice lacking PTEN in smooth muscle cells demonstrated sustained activation of Akt, upregulation of Runx2 with reductions in poly-ubiquitinated Runx2, and vascular calcification. Akt activation phosphorylated FoxO1/3a to promote nuclear extrusion of these molecules, producing the increase in

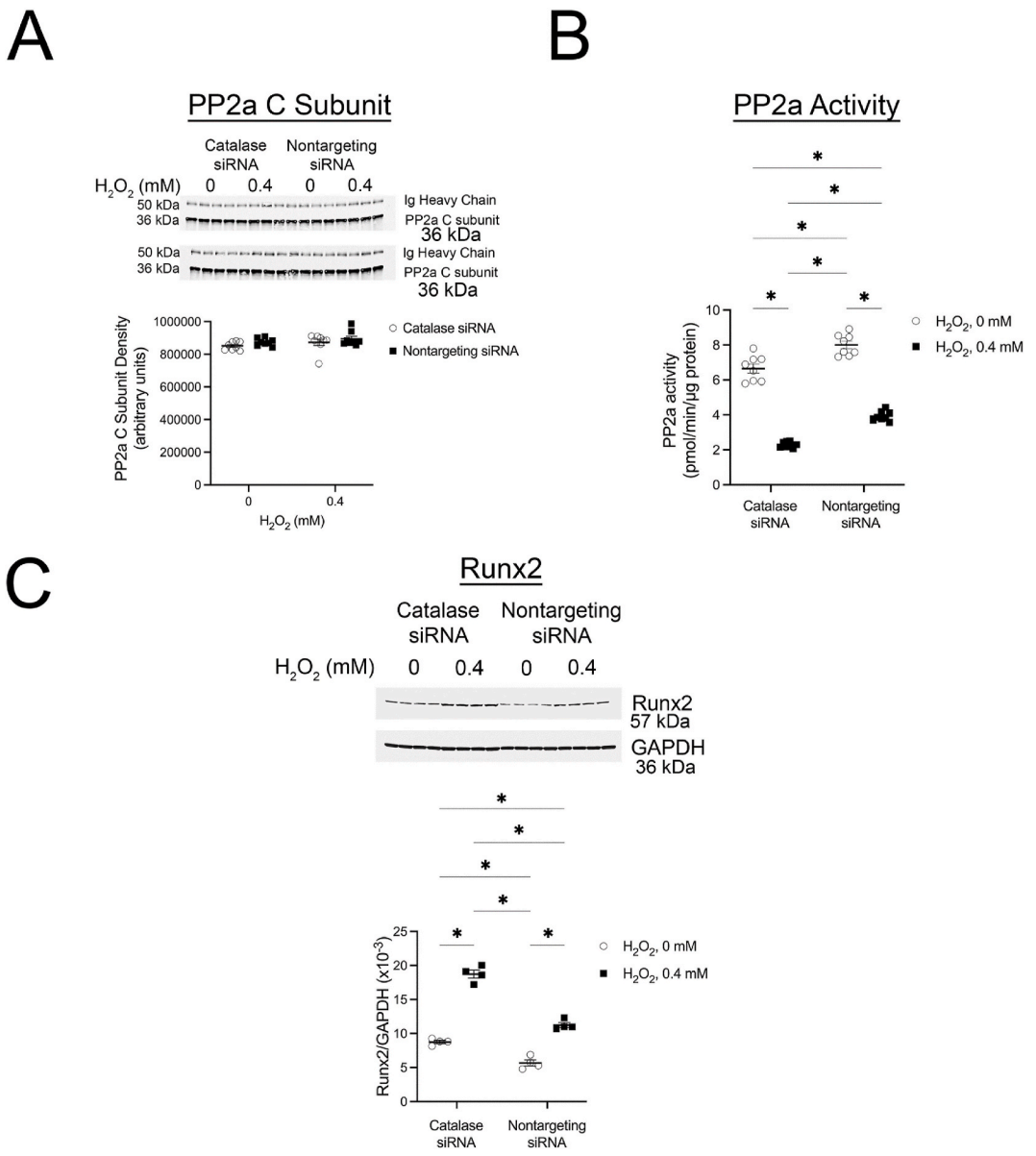

Fig. 10. Effect of siRNA-mediated knockdown of catalase on H_2O_2-induced decreases in PP2a activity and increases in Runx2 in VSMC. A and **B**, Immunoprecipitation of the active subunit of PP2a and subsequent analysis of PP2a activity in the immunoprecipitants showed that loss of catalase enhanced the effects of H_2O_2 on PP2a activity, but neither catalase knockdown nor H_2O_2 altered the amount of PP2a C subunit. In these experiments, H_2O_2 ($P < 0.05$) and catalase siRNA ($P < 0.05$) affected PP2a activity in VSMC but there was no interaction ($P > 0.05$) between H_2O_2 and catalase siRNA on PP2a activity. (n = 8 samples in each group; *$P < 0.05$; Two-way ANOVA) **C**, Knockdown of catalase enhanced the effects of H_2O_2 on Runx2 in VSMC. H_2O_2 ($P < 0.05$) and catalase siRNA ($P < 0.05$) affected Runx2 levels in VSMC and an interaction effect ($P < 0.05$) between H_2O_2 and catalase siRNA on Runx2 was observed. (n = 4 samples in each group; *$P < 0.05$; Two-way ANOVA).

Runx2 and subsequent osteogenic differentiation of VSMC [51]. In the current study, an increase in dietary NaCl also stimulated increased activity of Akt in lysates of aorta, along with increased phosphorylation of FoxO1 and FoxO3a. The direct involvement of this signaling pathway on Runx2 was strengthened by the in vitro studies that used pharmacological and biological inhibitors of members of this pathway. In addition, the unequivocal involvement of levels of FoxO1 and FoxO3a in determining Runx2 levels in VSMC was also congruent with a prior study that showed a post-transcriptional effect of FoxO1/3a on Runx2 in VSMC [51].

This study was also consistent with a prior series of experiments that examined a different environmental stress in kidney epithelial cells [35]. Immunoglobulin light chain protein catabolism by proximal tubule epithelium promoted a similar series of cell signaling events that occurred because of the generation of H_2O_2. That study featured the observation that Akt-mediated signaling through FoxO3a resulted in the downregulation of catalase, a critically important antioxidant enzyme [35]. Both studies now demonstrate augmentation of downstream redox-mediated events with reduction in catalase levels.

5. Conclusions

An increase in dietary salt intake initiated endothelial production of H_2O_2, uncovering interactions among Akt, FoxO1, FoxO3a, and sirtuin 1 in VSMC. These cellular responses to stress, with Akt serving an important counterregulatory factor by phosphorylating and inactivating the transcriptional activities of FoxO1 and FoxO3a, promoted a phenotypic switch with lowered catalase activity and increased Runx2 in

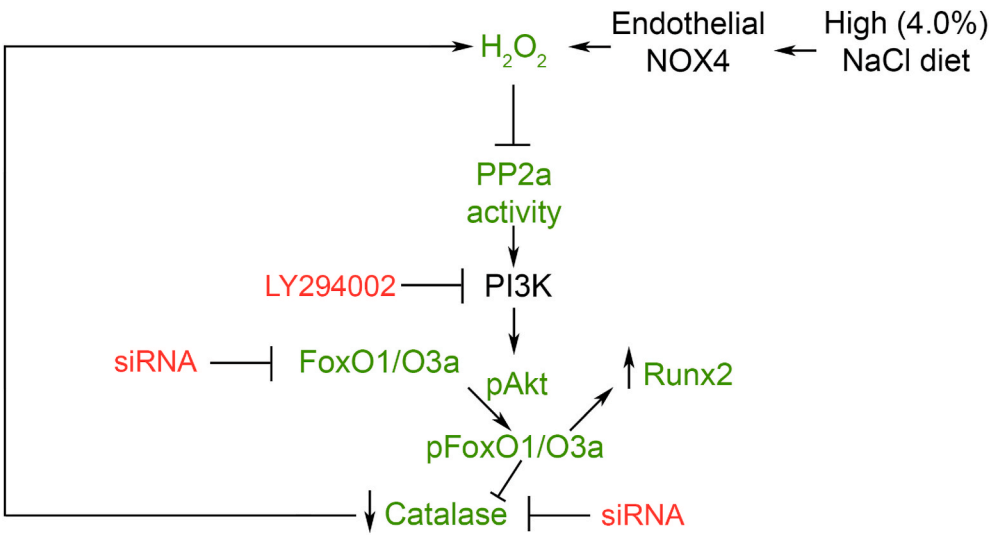

Fig. 11. Proposed redox-mediated endothelial cell-aortic smooth muscle cell communication. When fed a diet containing 4.0% NaCl, endothelial activity of NOX4 produced amounts of H_2O_2 sufficient to generate an endothelial cell-aortic smooth muscle cell communication that directly altered smooth muscle function. Specifically, reduction in PP2a activity promoted Akt activation and downstream inactivation of FoxO1 and FoxO3a. Stimulation of this important signaling pathway increased Runx2 and reduced catalase, which facilitated the activity of H_2O_2 and increased further Runx2 in aortic smooth muscle.

VSMC. One caveat to these results is that dietary potassium content was kept constant in these studies but has been shown to produce effects that may antagonize the adverse effects of dietary NaCl on endothelial and vascular smooth cell function [2,18]. An additional limitation of the present study was the lack of inclusion of a pathological endpoint, such as vascular calcification and aortic stiffness. In part, development of vascular pathology would promote changes in blood pressure, ensuring the introduction of a variable among the groups under study. Therefore, blood pressure was monitored using telemetry and the experiment was terminated prior to development of changes in blood pressure between the groups. The demonstrated increases in Runx2, osteopontin and osteocalcin supported the potential for development of vascular pathology, although these alterations in cellular physiology may be necessary but alone not sufficient to develop pathological changes. This concept was supported by studies that demonstrated the need to incubate cells in osteogenic medium along with H_2O_2 for three weeks to produce VSMC calcification in vitro [8]. Future efforts to accelerate vascular injury may require incorporation of models such as ApoE-deficient mice [18] or the recently described murine model of renovascular hypertension [57,58].

Authorship contributions

All authors assisted with the design of the study and participated in the acquisition and analysis of data. KY provided the initial draft of the manuscript. All authors revised and approved the final version of the manuscript.

Declaration of competing interests

Nothing to disclose.

Acknowledgments and funding support

This work was supported by a Merit Award (1 I01 BX005640) from the US Department of Veterans Affairs Basic Sciences R&D (BSRD) Service, a National Institutes of Health, National Institute of Diabetes and Digestive and Kidney Diseases George M. O'Brien Kidney and Urological Research Centers Program (2 P30 DK079337), and a UAB School of Medicine AMC21 Multi-PI Award. YC is supported by grants from the National Institutes of Health (5 R01 HL136165, 3 R01 HL146103, and 1 R01 HL158097) and from US Department of Veterans Affairs Basic Sciences R&D (BSRD) Service (1 IK6 BX005800 and 5 I01 BX004426).

Appendix A. Supplementary data

Supplementary data to this article can be found online at https://doi.org/10.1016/j.redox.2022.102296.

References

[1] V.P. Iyemere, D. Proudfoot, P.L. Weissberg, C.M. Shanahan, Vascular smooth muscle cell phenotypic plasticity and the regulation of vascular calcification, J. Intern. Med. 260 (3) (2006) 192–210, https://doi.org/10.1111/j.1365-2796.2006.01692.x.

[2] W.Z. Ying, K.J. Aaron, P.W. Sanders, Effect of aging and dietary salt and potassium intake on endothelial PTEN (Phosphatase and tensin homolog on chromosome 10) function, PLoS One 7 (11) (2012), e48715, https://doi.org/10.1371/journal.pone.0048715.

[3] M.A. Engelse, J.M. Neele, A.L. Bronckers, H. Pannekoek, C.J. de Vries, Vascular calcification: expression patterns of the osteoblast-specific gene core binding factor alpha-1 and the protective factor matrix gla protein in human atherogenesis, Cardiovasc. Res. 52 (2) (2001) 281–289, https://doi.org/10.1016/s0008-6363(01)00375-3.

[4] E. Aikawa, M. Nahrendorf, J.L. Figueiredo, F.K. Swirski, T. Shtatland, R.H. Kohler, F.A. Jaffer, M. Aikawa, R. Weissleder, Osteogenesis associates with inflammation in early-stage atherosclerosis evaluated by molecular imaging in vivo, Circulation 116 (24) (2007) 2841–2850.

[5] K.L. Tyson, J.L. Reynolds, R. McNair, Q. Zhang, P.L. Weissberg, C.M. Shanahan, Osteo/chondrocytic transcription factors and their target genes exhibit distinct patterns of expression in human arterial calcification, Arterioscler. Thromb. Vasc. Biol. 23 (3) (2003) 489–494, https://doi.org/10.1161/01.ATV.0000059406.92165.31.

[6] P. Ducy, R. Zhang, V. Geoffroy, A.L. Ridall, G. Karsenty, Osf2/Cbfa1: a transcriptional activator of osteoblast differentiation, Cell 89 (5) (1997) 747–754, https://doi.org/10.1016/s0092-8674(00)80257-3.

[7] J.B. Lian, A. Javed, S.K. Zaidi, C. Lengner, M. Montecino, A.J. van Wijnen, J. L. Stein, G.S. Stein, Regulatory controls for osteoblast growth and differentiation: role of Runx/Cbfa/AML factors, Crit. Rev. Eukaryot. Gene Expr. 14 (1–2) (2004) 1–41.

[8] C.H. Byon, A. Javed, Q. Dai, J.C. Kappes, T.L. Clemens, V.M. Darley-Usmar, J. M. McDonald, Y. Chen, Oxidative stress induces vascular calcification through modulation of the osteogenic transcription factor Runx2 by AKT signaling, J. Biol. Chem. 283 (22) (2008) 15319–15327.

[9] Y. Sun, C.H. Byon, K. Yuan, J. Chen, X. Mao, J.M. Heath, A. Javed, K. Zhang, P. G. Anderson, Y. Chen, Smooth muscle cell-specific runx2 deficiency inhibits vascular calcification, Circ. Res. 111 (5) (2012) 543–552, https://doi.org/10.1161/CIRCRESAHA.112.267237.

[10] U. Raaz, I.N. Schellinger, E. Chernogubova, C. Warnecke, Y. Kayama, K. Penov, J. K. Hennigs, F. Salomons, S. Eken, F.C. Emrich, W.H. Zheng, M. Adam, A. Jagger, F. Nakagami, R. Toh, K. Toyama, A. Deng, M. Buerke, L. Maegdefessel, G. Hasenfuss, J.M. Spin, P.S. Tsao, Transcription factor Runx2 promotes aortic fibrosis and stiffness in type 2 Diabetes mellitus, Circ. Res. 117 (6) (2015) 513–524, https://doi.org/10.1161/CIRCRESAHA.115.306341.

[11] E.G. Lakatta, Arterial and cardiac aging: major shareholders in cardiovascular disease enterprises: Part III: cellular and molecular clues to heart and arterial aging, Circulation 107 (3) (2003) 490–497.

[12] S.E. Greenwald, Ageing of the conduit arteries, J. Pathol. 211 (2) (2007) 157–172, https://doi.org/10.1002/path.2101.

[13] M.F. O'Rourke, M.E. Safar, Relationship between aortic stiffening and microvascular disease in brain and kidney: cause and logic of therapy, Hypertension 46 (1) (2005) 200–204.

[14] P. Fesler, M.E. Safar, G. du Cailar, J. Ribstein, A. Mimran, Pulse pressure is an independent determinant of renal function decline during treatment of essential hypertension, J. Hypertens. 25 (9) (2007) 1915–1920.

[15] Y. Ben-Shlomo, M. Spears, C. Boustred, M. May, S.G. Anderson, E.J. Benjamin, P. Boutouyrie, J. Cameron, C.H. Chen, J.K. Cruickshank, S.J. Hwang, E.G. Lakatta, S. Laurent, J. Maldonado, G.F. Mitchell, S.S. Najjar, A.B. Newman, M. Ohishi, B. Pannier, T. Pereira, R.S. Vasan, T. Shokawa, K. Sutton-Tyrell, F. Verbeke, K. L. Wang, D.J. Webb, T. Willum Hansen, S. Zoungas, C.M. McEniery, J.R. Cockcroft, I.B. Wilkinson, Aortic pulse wave velocity improves cardiovascular event prediction: an individual participant meta-analysis of prospective observational data from 17,635 subjects, J. Am. Coll. Cardiol. 63 (7) (2014) 636–646, https://doi.org/10.1016/j.jacc.2013.09.063.

[16] T.J. Niiranen, A. Lyass, M.G. Larson, N.M. Hamburg, E.J. Benjamin, G.F. Mitchell, R.S. Vasan, Prevalence, correlates, and prognosis of healthy vascular aging in a western community-dwelling cohort: the framingham heart study, Hypertension 70 (2) (2017) 267–274, https://doi.org/10.1161/HYPERTENSIONAHA.117.09026.

[17] T. Willum-Hansen, J.A. Staessen, C. Torp-Pedersen, S. Rasmussen, L. Thijs, H. Ibsen, J. Jeppesen, Prognostic value of aortic pulse wave velocity as index of arterial stiffness in the general population, Circulation 113 (5) (2006) 664–670, https://doi.org/10.1161/CIRCULATIONAHA.105.579342.

[18] Y. Sun, C.H. Byon, Y. Yang, W.E. Bradley, L.J. Dell'Italia, P.W. Sanders, A. Agarwal, H. Wu, Y. Chen, Dietary potassium regulates vascular calcification and arterial stiffness, JCI insight 2 (19) (2017), https://doi.org/10.1172/jci.insight.94920.

[19] W.Z. Ying, P.W. Sanders, Dietary salt modulates renal production of transforming growth factor-beta in rats, Am. J. Physiol. 274 (4 Pt 2) (1998) F635–F641.

[20] W.-Z. Ying, P.W. Sanders, Increased dietary salt activates rat aortic endothelium, Hypertension 39 (2002) 239–244.

[21] W.Z. Ying, K. Aaron, P.X. Wang, P.W. Sanders, Potassium inhibits dietary salt-induced transforming growth factor-beta production, Hypertension 54 (5) (2009) 1159–1163. HYPERTENSIONAHA.109.138255 [pii] 10.1161/HYPERTENSIONAHA.109.138255.

[22] W.Z. Ying, K.J. Aaron, P.W. Sanders, Transforming growth factor-β regulates endothelial function during high salt intake in rats, Hypertension 62 (2013) 951–956, https://doi.org/10.1161/HYPERTENSIONAHA.113.01835.

[23] W.Z. Ying, K.J. Aaron, P.W. Sanders, Sodium and potassium regulate endothelial phospholipase C-gamma and Bmx, Am. J. Physiol. Ren. Physiol. 307 (1) (2014) F58–F63, https://doi.org/10.1152/ajprenal.00615.2013.

[24] A.P. Avolio, K.M. Clyde, T.C. Beard, H.M. Cooke, K.K. Ho, M.F. O'Rourke, Improved arterial distensibility in normotensive subjects on a low salt diet, Arteriosclerosis 6 (2) (1986) 166–169.

[25] P.E. Gates, H. Tanaka, W.R. Hiatt, D.R. Seals, Dietary sodium restriction rapidly improves large elastic artery compliance in older adults with systolic hypertension, Hypertension 44 (1) (2004) 35–41.

[26] P.F. Davies, Flow-mediated endothelial mechanotransduction, Physiol. Rev. 75 (1995) 519–560.

[27] M. Ohno, G.H. Gibbons, V.J. Dzau, J.P. Cooke, Shear stress elevates endothelial cGMP. Role of a potassium channel and G protein coupling, Circulation 88 (1) (1993) 193–197.

[28] W. Feng, W.Z. Ying, K.J. Aaron, P.W. Sanders, Transforming growth factor-beta mediates endothelial dysfunction in rats during high salt intake, Am. J. Physiol. Ren. Physiol. 309 (12) (2015) F1018–F1025, https://doi.org/10.1152/ajprenal.00328.2015.

[29] H.S. Marinho, C. Real, L. Cyrne, H. Soares, F. Antunes, Hydrogen peroxide sensing, signaling and regulation of transcription factors, Redox Biol. 2 (2014) 535–562, https://doi.org/10.1016/j.redox.2014.02.006.

[30] C.H. Byon, J.M. Heath, Y. Chen, Redox signaling in cardiovascular pathophysiology: a focus on hydrogen peroxide and vascular smooth muscle cells, Redox Biol 9 (2016) 244–253, https://doi.org/10.1016/j.redox.2016.08.015.

[31] Y. Nisimoto, B.A. Diebold, D. Cosentino-Gomes, J.D. Lambeth, Nox4: a hydrogen peroxide-generating oxygen sensor, Biochemistry 53 (31) (2014) 5111–5120, https://doi.org/10.1021/bi500331y.

[32] K.D. Martyn, L.M. Frederick, K. von Loehneysen, M.C. Dinauer, U.G. Knaus, Functional analysis of Nox4 reveals unique characteristics compared to other NADPH oxidases, Cell. Signal. 18 (1) (2006) 69–82, https://doi.org/10.1016/j.cellsig.2005.03.023.

[33] Q. Xu, A.A. Kulkarni, A.M. Sajith, D. Hussein, D. Brown, O.F. Guner, M.D. Reddy, E. B. Watkins, B. Lassegue, K.K. Griendling, J.P. Bowen, Design, synthesis, and biological evaluation of inhibitors of the NADPH oxidase, Nox4, Bioorg. Med. Chem. 26 (5) (2018) 989–998, https://doi.org/10.1016/j.bmc.2017.12.023.

[34] T. Ago, T. Kitazono, H. Ooboshi, T. Iyama, Y.H. Han, J. Takada, M. Wakisaka, S. Ibayashi, H. Utsumi, M. Iida, Nox4 as the major catalytic component of an endothelial NAD(P)H oxidase, Circulation 109 (2) (2004) 227–233, https://doi.org/10.1161/01.CIR.0000105680.92873.70.

[35] K.E. Ying, W. Feng, W.Z. Ying, P.W. Sanders, Cellular antioxidant mechanisms control immunoglobulin light chain-mediated proximal tubule injury, Free Radic. Biol. Med. 171 (2021) 80–90, https://doi.org/10.1016/j.freeradbiomed.2021.05.011.

[36] K. Okumoto, M. El Shermely, M. Natsui, H. Kosako, R. Natsuyama, T. Marutani, Y. Fujiki, The peroxisome counteracts oxidative stresses by suppressing catalase import via Pex14 phosphorylation, Elife 9 (2020), https://doi.org/10.7554/eLife.55896.

[37] C.J. Vlahos, W.F. Matter, K.Y. Hui, R.F. Brown, A specific inhibitor of phosphatidylinositol 3-kinase, 2-(4-morpholinyl)-8-phenyl-4H-1-benzopyran-4-one (LY294002), J. Biol. Chem. 269 (7) (1994) 5241–5248.

[38] R. Radi, J.S. Beckman, K.M. Bush, B.A. Freeman, Peroxynitrite oxidation of sulfhydryls. The cytotoxic potential of superoxide and nitric oxide, J. Biol. Chem. 266 (7) (1991) 4244–4250.

[39] S.W. Ballinger, C. Patterson, C.N. Yan, R. Doan, D.L. Burow, C.G. Young, F. M. Yakes, B. Van Houten, C.A. Ballinger, B.A. Freeman, M.S. Runge, Hydrogen peroxide- and peroxynitrite-induced mitochondrial DNA damage and dysfunction in vascular endothelial and smooth muscle cells, Circ. Res. 86 (9) (2000) 960–966, https://doi.org/10.1161/01.res.86.9.960.

[40] C. Cseko, Z. Bagi, A. Koller, Biphasic effect of hydrogen peroxide on skeletal muscle arteriolar tone via activation of endothelial and smooth muscle signaling pathways, J. Appl. Physiol. 97 (3) (2004) 1130–1137, https://doi.org/10.1152/japplphysiol.00106.2004, 1985.

[41] N. Mody, F. Parhami, T.A. Sarafian, L.L. Demer, Oxidative stress modulates osteoblastic differentiation of vascular and bone cells, Free Radic. Biol. Med. 31 (4) (2001) 509–519, https://doi.org/10.1016/s0891-5849(01)00610-4.

[42] M. Zana, Z. Peterfi, H.A. Kovacs, Z.E. Toth, B. Enyedi, F. Morel, M.H. Paclet, A. Donko, S. Morand, T.L. Leto, M. Geiszt, Interaction between p22(phox) and Nox4 in the endoplasmic reticulum suggests a unique mechanism of NADPH oxidase complex formation, Free Radic. Biol. Med. 116 (2018) 41–49, https://doi.org/10.1016/j.freeradbiomed.2017.12.031.

[43] L. Hecker, R. Vittal, T. Jones, R. Jagirdar, T.R. Luckhardt, J.C. Horowitz, S. Pennathur, F.J. Martinez, V.J. Thannickal, NADPH oxidase-4 mediates myofibroblast activation and fibrogenic responses to lung injury, Nat. Med. 15 (9) (2009) 1077–1081, https://doi.org/10.1038/nm.2005.

[44] V.J. Thannickal, P.M. Hassoun, A.C. White, B.L. Fanburg, Enhanced rate of H2O2 release from bovine pulmonary artery endothelial cells induced by TGF-beta 1, Am. J. Physiol. 265 (6 Pt 1) (1993) L622–L626.

[45] A. Martin-Garrido, D.I. Brown, A.N. Lyle, A. Dikalova, B. Seidel-Rogol, B. Lassegue, A. San Martin, K.K. Griendling, NADPH oxidase 4 mediates TGF-beta-induced smooth muscle alpha-actin via p38MAPK and serum response factor, Free Radic. Biol. Med. 50 (2) (2011) 354–362, https://doi.org/10.1016/j.freeradbiomed.2010.11.007.

[46] A. Lozhkin, A.E. Vendrov, H. Pan, S.A. Wickline, N.R. Madamanchi, M.S. Runge, NADPH oxidase 4 regulates vascular inflammation in aging and atherosclerosis, J. Mol. Cell. Cardiol. 102 (2017) 10–21, https://doi.org/10.1016/j.yjmcc.2016.12.004.

[47] U. Rauen, T. Li, I. Ioannidis, H. de Groot, Nitric oxide increases toxicity of hydrogen peroxide against rat liver endothelial cells and hepatocytes by inhibition of hydrogen peroxide degradation, Am. J. Physiol. Cell Physiol. 292 (4) (2007) C1440–C1449, https://doi.org/10.1152/ajpcell.00366.2006.

[48] G. Bauer, Increasing the endogenous NO level causes catalase inactivation and reactivation of intercellular apoptosis signaling specifically in tumor cells, Redox Biol. 6 (2015) 353–371, https://doi.org/10.1016/j.redox.2015.07.017.

[49] S. Ghosh, A.J. Janocha, M.A. Aronica, S. Swaidani, S.A. Comhair, W. Xu, L. Zheng, S. Kaveti, M. Kinter, S.L. Hazen, S.C. Erzurum, Nitrotyrosine proteome survey in asthma identifies oxidative mechanism of catalase inactivation, J. Immunol. 176 (9) (2006) 5587–5597, https://doi.org/10.4049/jimmunol.176.9.5587.

[50] A. Brunet, A. Bonni, M.J. Zigmond, M.Z. Lin, P. Juo, L.S. Hu, M.J. Anderson, K. C. Arden, J. Blenis, M.E. Greenberg, Akt promotes cell survival by phosphorylating and inhibiting a Forkhead transcription factor, Cell 96 (6) (1999) 857–868, https://doi.org/10.1016/s0092-8674(00)80595-4.

[51] L. Deng, L. Huang, Y. Sun, J.M. Heath, H. Wu, Y. Chen, Inhibition of FOXO1/3 promotes vascular calcification, Arterioscler. Thromb. Vasc. Biol. 35 (1) (2015) 175–183, https://doi.org/10.1161/ATVBAHA.114.304786.

[52] G. Tzivion, M. Dobson, G. Ramakrishnan, FoxO transcription factors; Regulation by AKT and 14-3-3 proteins, Biochim. Biophys. Acta 1813 (11) (2011) 1938–1945, https://doi.org/10.1016/j.bbamcr.2011.06.002.

[53] D. Accili, K.C. Arden, FoxOs at the crossroads of cellular metabolism, differentiation, and transformation, Cell 117 (4) (2004) 421–426, https://doi.org/10.1016/s0092-8674(04)00452-0.

[54] A. Takai, M. Eto, K. Hirano, K. Takeya, T. Wakimoto, M. Watanabe, Protein phosphatases 1 and 2A and their naturally occurring inhibitors: current topics in smooth muscle physiology and chemical biology, J. Physiol. Sci. 68 (1) (2018) 1–17, https://doi.org/10.1007/s12576-017-0556-6.

[55] F. Rusnak, T. Reiter, Sensing electrons: protein phosphatase redox regulation, Trends Biochem. Sci. 25 (11) (2000) 527–529, https://doi.org/10.1016/s0968-0004(00)01659-5.

[56] R.K. Rao, L.W. Clayton, Regulation of protein phosphatase 2A by hydrogen peroxide and glutathionylation, Biochem. Biophys. Res. Commun. 293 (1) (2002) 610–616, https://doi.org/10.1016/S0006-291X(02)00268-1.

[57] J.C. Galley, S.A. Hahn, M.P. Miller, B.G. Durgin, E.K. Jackson, S.D. Stocker, A. C. Straub, Angiotensin II augments renal vascular smooth muscle soluble GC expression via an AT1 receptor-forkhead box subclass O transcription factor signalling axis, Br. J. Pharmacol. (2021), https://doi.org/10.1111/bph.15522.

[58] L.J. DeLalio, S. Hahn, P.L. Katayama, M.M. Wenner, W.B. Farquhar, A.C. Straub, S. D. Stocker, Excessive dietary salt promotes aortic stiffness in murine renovascular hypertension, Am. J. Physiol. Heart Circ. Physiol. 318 (5) (2020) H1346–H1355, https://doi.org/10.1152/ajpheart.00601.2019.